Electronic and Molecular Structure of Variable-Spin Iron(III) Chelates with Hexadentate Ligands Derived from Triethylenetetramine and β-Diketones or Salicylaldehyde. Spin State Dependent Crystal and Molecular Structures of $[Fe(acac)_2trien]PF_6$ ($S = 5/2$), $[Fe(acacCl)_2trien]PF_6$ ($S = 5/2$), $[Fe(sal)_2trien]Cl\cdot 2H_2O$ ($S = 1/2$), and $[Fe(sal)_2trien]NO_3\cdot H_2O$ ($S = 1/2$)

Ekk Sinn,*[1] Greig Sim,[1] Eric V. Dose,[2] Michael F. Tweedle,[2] and Lon J. Wilson*[3]

Contribution from the Department of Chemistry, University of Virginia, Charlottesville, Virginia 22901, and the Department of Chemistry, William Marsh Rice University, Houston, Texas 77001. *Received June 10, 1977*

Abstract: Six-coordinate iron(III) complexes derived from triethylenetetramine (trien) and acetylacetone (acac), 3-chloroacetylacetone (acacCl), or salicylaldehyde (sal), $[Fe(acac)_2trien](X)$, $[Fe(acacCl)_2trien](PF_6)$, and $[Fe(sal)_2trien](Y)$ (X = PF_6^-, BPh_4^-; Y = PF_6^-, Cl^-, NO_3^-) have been shown by variable-temperature magnetochemical and Mössbauer spectroscopy measurements to be members of a family of low-spin ($S = 1/2$; $^2T_2$) ⇄ high-spin ($S = 5/2$; $^6A_1$) spin-equilibrium compounds in the solid state. The acac and acacCl compounds with X = PF_6^- are essentially high spin (~5.9 μ_B) at room temperature, whereas the sal complexes with Y = $Cl^-\cdot 2H_2O$ and $NO_3^-\cdot H_2O$) are mainly low spin (1.94 and 2.47 μ_B). X-ray crystallographic structure determinations of these four compounds show that, except for the differences between the acac, acacCl, and sal ligand moieties, the cations possess the same general structures with an N_4O_2 donor atom set of a hexadentate ligand forming a distorted octahedron about the metal atom. In each case the terminal oxygen donor atoms occupy cis positions and the remaining four nitrogen atoms (two cis amine and two trans imine) complete the coordinate sphere. The fine structural details for the four compounds reveal significant differences in the metal atom environments which can be largely attributed to the differing $S = 5/2$ and $S = 1/2$ spin states. For the $S = 1/2$ sal complexes, the average metal-ligand bond length (δ_{av}) is shorter by about 0.12–0.13 Å relative to the $S = 5/2$ cases, but this difference is not uniform: the Fe–N bonds vary far more [δ(amine) 0.17 Å; δ(imine) 0.17 Å] than the Fe–O bonds (δ 0.04 Å). In the low-spin $[Fe(sal)_2trien]Cl\cdot 2H_2O$ complex, the Cl^- ion is hydrogen bonded to the two water molecules, one of which is in turn hydrogen bonded to an amine donor atom; this hydrogen bonding network in the solid state is consistent with earlier solution state studies where strong [solvent···HN] interactions were shown to promote the low-spin state. The hydrogen bonding forms a polymeric chain of anions and cations. A similar hydrogen bonding scheme also exists in the low-spin NO_3^- compound. The spin state dependent structural changes observed for the present spin-equilibrium system are compared to those for the electronically similar, but structurally different, tris(dithiocarbamato)-iron(III) complexes, and the possible consequences of these spin-related structural changes discussed in terms of molecular volume and dynamic spin lifetime measurements in the solution state. Crystal data for $[Fe(acac)_2trien]PF_6$: $FePF_6O_2N_4C_{16}H_{28}$, space group $C2/c$, $Z = 8$, $a = 24.44$ (1) Å, $b = 13.315$ (6) Å, $c = 15.202$ (7) Å, $\beta = 113.51$ (3)°, $V = 4536$ Å^3, $R = 5.5\%$, 2849 reflections. Crystal data for $[Fe(acacCl)_2trien]PF_6$: $FeCl_2PF_6O_2N_4C_{16}H_{26}$, space group $C2/c$, $Z = 8$, $a = 24.14$ (1) Å, $b = 13.404$ (9) Å, $c = 15.98$ (1) Å, $\beta = 111.56$ (7)°, $V = 4810$ Å^3, $R = 6.7\%$, 1186 reflections. Crystal data for $[Fe(sal)_2trien]Cl\cdot 2H_2O$: $FeClO_4N_4C_{20}H_{28}$, space group $P2_1/c$, $Z = 4$, $a = 18.58$ (1) Å, $b = 10.026$ (3) Å, $c = 12.061$ (5) Å, $\beta = 103.28$ (3)°, $V = 2187$ Å^3, $R = 3.4\%$ 2614 reflections. Crystal data for $[Fe(sal)_2trien]NO_3\cdot H_2O$: $FeO_6N_5C_{20}H_{26}$, space group $P2_1/a$, $Z = 4$, $a = 11.979$ (7) Å, $b = 9.967$ (4) Å, $c = 18.472$ (7) Å, $\beta = 98.38$ (5)°, $V = 2182$ Å^3, $R = 4.5\%$, 2408 reflections.

Introduction

Metal complexes such as the ferric dithiocarbamates, which exhibit low-spin ($^2T_2$) ⇄ high-spin ($^6A_1$) spin equilibria, have properties dependent on the proportion of high-spin and low-spin species present and this proportion is sensitive to temperature, pressure, and slight chemical modifications.[4] Magnetic susceptibility measurements on ferric dithiocarbamates in solution at pressures from 1 to 3000 atm have shown the low-spin species to be smaller in volume than the high-spin by 5–6 cm^3/mol.[4] This observation has been further substantiated by x-ray crystallographic studies on ferric dithiocarbamates with various ligand substituents, which show that in general a shorter metal–ligand bond length is observed as the proportion of low-spin species increases, even though complexes somewhat chemically different are involved.[5–12] A crystallographic study of the tris(diethyldithiocarbamato)iron(III) species at two different temperatures (80, 296 K) has demonstrated a decrease of 0.05 Å for an approximately 45% shift toward the low-spin side of the equilibrium.[13] It should be noted, however, that variable-temperature studies are sometimes unnecessary for such spin state dependent structural investigations, since recrystallization from different solvents can cause a shift in the equilibrium as great as pressure changes of several thousand atmospheres or temperature changes of several hundred degrees,[9–12,14,15] with these occluded-solvent induced shifts in the equilibrium being accompanied by the expected change in metal–ligand bond length at room temperature. For only two iron(II)[18,19,20] and the above-mentioned iron(III) complexes has the metal–ligand bond length change for spin state crossover processes been investigated, and only in the iron(III) dithiocarbamate case has it been studied in any detail. Since the magnitude and pattern of such metal–ligand bond distances changes accompanying spin conversion are of fundamental interest in both inorganic transition metal chemistry[21] and heme metalloprotein chemistry,[22] there is a decided need for more extensive documentation of the phenomenon. In particular, it has recently been suggested[23] that measured rate constants for (low-spin) ⇄ (high-spin) spin interconversion in spin-equilibrium Fe(II),[24,25] Fe(III),[16,17]

0002-7863/78/1500-3375$01.00/0

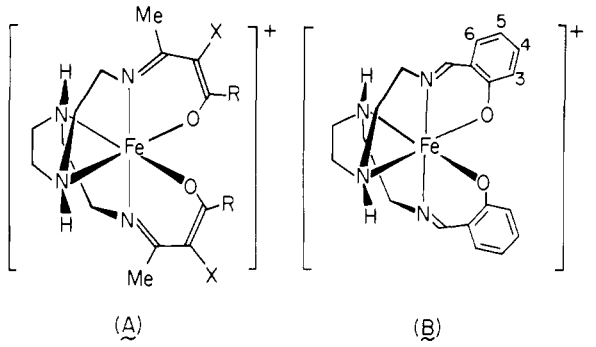

(A) (B)

Figure 1. General structures of the variable-spin iron(III) cations: $[Fe(acac)_2trien]^+$ (A with R = Me, X = H), $[Fe(acacCl)_2trien]^+$ (A with R = Me, X = Cl), and $[Fe(sal)_2trien)]^+$ (B).

and Co(II)[26] complexes may be largely rate determined by the nature and extent of the coordination sphere reorganization processes which result from the change in spin multiplicity.

In this work we wish to report the magnetic, Mössbauer, and structural properties of the $[Fe(acac)_2trien]^+$, $[Fe(acacCl)_2trien]^+$, and $[Fe(sal)_2trien]^+$ cations (Figure 1) which are low-spin ($S = ½$) ⇄ high-spin ($S = 5/2$) iron(III) species in the solid state. The solution state properties of the spin equilibria have been reported earlier.[16,17] The room temperature x-ray structural determinations for four of the compounds, $[Fe(acac)_2trien](PF_6)$, $[Fe(acacCl)_2trien](PF_6)$, $[Fe(sal)_2trien]Cl·2H_2O$, and $[Fe(sal)_2trien]NO_3·H_2O$, are of particular interest since the acac and acacCl PF_6^- salts are both essentially high-spin structures, while the sal derivatives are mainly low spin. Furthermore, structural comparisons of these ($S = ½$) ⇄ ($S = 5/2$) spin-equilibrium compounds to those for the much-studied tris(dithiocarbamato)iron(III) complexes are especially noteworthy since, except for the spin-equilibrium property, the two systems have little else in common. The trien complexes are ionic, based on hexadentate ligands, and contain only nitrogen and oxygen ligand donor atoms, while the $Fe(dtc)_3$'s are uncharged, tris bidentates, and contain only sulfur donor atoms. Thus, properties in common between the two different systems of complexes can largely be ascribed to spin state equilibrium phenomena.

Experimental Section

Syntheses of the compounds were carried out as described previously,[16,17] except for the sample of $[Fe(sal)_2trien]Cl·2H_2O$ used for the crystal structure determinations. Magnetic susceptibilities were measured by the Faraday method using a Cahn Model 6600-1 Research Magnetic Susceptibility System and $Hg[Co(NCS)_4]$ as the calibrant. The cryogenics consisted of an Air Products Faraday Interface Model DMX-19 Vacuum Shroud, an LT-3-110B Heli-tran system, and an APD-TL Digital Temperature Readout monitoring an iron-doped gold vs. chromel thermocouple.[41] The thermocouple was calibrated using susceptibility vs. temperature data for the $Hg[Co(NCS)_4]$ calibrant compound.[27] Mössbauer spectra were taken on equipment previously described using sodium nitroprusside as a calibrant and the data analyzed by means of a standard Mössbauer computer fitting program.[16] The temperature was measured by a copper constantan thermocouple imbedded in the sample.

Suitable single crystals of $[Fe(acac)_2trien](PF_6)$ were obtained by preparing a nearly saturated solution in dichloromethane, adding dropwise an equal volume of *n*-heptane, and allowing the mixture to stand. Crystals of $[Fe(sal)_2trien]Cl·2H_2O$ were prepared as follows: 1,8-diamino-3,6-diazaoctane tetrahydrochloride [trien·4HCl] was suspended in methanol (20 mL) and $NaOCH_3$ (1.62 g) added with stirring. The suspension was stirred for 30 min, then filtered. Salicylaldehyde (3.7 g) was added and the mixture refluxed for 20 min. $FeCl_3·6H_2O$ (2.7 g) was added, and then a further 1.62 g of $NaOCH_3$ was added to the refluxing solution. The mixture was refluxed for 10 min, then the methanol was removed by rotary evaporation. Dichloromethane (20 mL) was added to the flask and refluxed for 15 min. The solution was filtered hot and crystals of the complex separated on cooling.

Crystal data for $[Fe(acac)_2trien]PF_6$: $FePF_6O_2N_4C_{16}H_{28}$, mol wt 509, space group $C2/c$, $Z = 8$, $a = 24.44$ (1) Å, $b = 13.315$ (6) Å, $c = 15.202$ (7) Å, $\beta = 113.51$ (3)°, $V = 4536$ Å^3, $R = 5.5\%$, 2849 reflections, μ(Mo Kα) = 8.3 cm^{-1}, $\rho_{calcd} = 1.46$ g cm^{-3}, $\rho_{obsd} = 1.47$ g cm^{-3}; crystal dimensions (distance in mm from centroid) (101) 0.07, ($\bar{1}0\bar{1}$) 0.07, (010) 0.08, (0$\bar{1}$0) 0.08, (10$\bar{1}$) 0.50, ($\bar{1}$01) 0.50.

Crystal data for $[Fe(acacCl)_2trien]PF_6$: $FeCl_2PF_6O_2N_4C_{16}H_{26}$, mol wt 578, space group $C2/c$, $Z = 8$, $a = 24.14$ (1) Å, $b = 13.404$ (9) Å, $c = 15.98$ (1) Å, $\beta = 111.56$ (7)°, $V = 4810$ Å^3, 1186 reflections, μ(Mo Kα) = 10.1 cm^{-1}, $\rho_{calcd} = 1.60$ g cm^{-3}, $\rho_{obsd} = 1.62$ g cm^{-3}; crystal dimensions (mm from centroid) (100) 0.20, ($\bar{1}$00) 0.20, (101) 0.08, ($\bar{1}0\bar{1}$) 0.08, (111) 0.08, ($\bar{1}\bar{1}\bar{1}$) 0.08.

Crystal data for $[Fe(sal)_2trien]Cl·2H_2O$: $FeClO_4N_4C_{20}H_{28}$, mol wt 480, space group $P2_1/c$, $Z = 4$, $a = 18.58$ (1) Å, $b = 10.026$ (3) Å, $c = 12.061$ (5) Å, $\beta = 103.28$ (3)°, $V = 2187$ Å^3, $R = 3.4\%$, 2614 reflections, μ(Mo Kα) = 8.7 cm^{-1}, $\rho_{calcd} = 1.47$, $\rho_{obsd} = 1.46$ g cm^{-3}; crystal dimensions (mm from centroid) (100) 0.035, ($\bar{1}$00) 0.035, (0$\bar{1}\bar{1}$) 0.37, (01$\bar{1}$) 0.37, (0$\bar{1}\bar{1}$) 0.39, (011) 0.39, (001) 0.18, (00$\bar{1}$) 0.18.

Crystal data $[Fe(sal)_2trien]NO_3·H_2O$: $FeO_6N_5C_{20}H_{26}$, mol wt 489, space group $P2_1/a$, $Z = 4$, $a = 11.979$ (7) Å, $b = 9.967$ (4) Å, $c = 18.472$ (7) Å, $\beta = 98.38$ (5)°, $V = 2182$ Å^3, μ(Mo Kα) = 7.6 cm^{-1}, $\rho_{calcd} = 1.49$ g cm^{-3}, $\rho_{obsd} = 1.48$ g cm^{-3}; crystal dimensions (mm from centroid) (1$\bar{1}$0) 0.17, ($\bar{1}$10) 0.17, ($\bar{1}\bar{1}$0) 0.10, (22$\bar{3}$) 0.10, (001) 0.13, (00$\bar{1}$) 0.13.

For each crystal, the Enraf-Nonius program SEARCH was used to obtain 15 accurately centered reflections which were then used in the program INDEX to obtain approximate cell dimensions and an orientation matrix for data collection. Refined cell dimensions and their estimated standard deviations were obtained from least-squares refinement of 28 accurately centered reflections. The mosaicity of each crystal was examined by the ω-scan technique and judged to be satisfactory.

Diffraction data were collected at 292 K on an Enraf-Nonius four-circle CAD-4 diffractometer controlled by a PDP8/M computer, using Mo Kα radiation from a highly oriented graphite crystal monochromator. The θ-2θ scan technique was used to record the intensities for all nonequivalent reflections for which $1° < 2\theta < 46°$ for $[Fe(acac)_2trien)]PF_6$ and $[Fe(sal)_2trien)]Cl·2H_2O$ and $1° < 2\theta < 42°$ for $[Fe(acacCl)_2trien]PF_6$. Scan widths (SW) were calculated from the formula $SW = A + B \tan\theta$ where A is estimated from the mosaicity of the crystal and B allows for the increase in width of peak due to Kα_1 and Kα_2 splitting. The values of A and B were 0.60 and 0.30°, respectively, in each case. The calculated scan angle is extended on each side by 25% for background determination (BG1 and BG2). The net count is then calculated as NC = TOT − 2(BG1 + BG2), where TOT is the integrated peak intensity. Reflection data were considered insignificant if intensities registered less than 5 counts above background on a rapid prescan, such reflections being rejected automatically by the computer.

The intensities of four standard reflections, monitored at 100 reflection intervals, showed no greater fluctuations during the data collection than those expected from Poisson statistics. The raw intensity data were corrected for Lorentz-polarization effects (including the polarization effect of the crystal monochromator) and then for absorption. After averaging the intensities of equivalent reflections, the data were reduced to 2958 independent intensities for $[Fe(acac)_2trien]PF_6$, 2158 for $[Fe(acacCl)_2trien]PF_6$, 3428 for $[Fe(sal)_2trien]Cl·2H_2O$, and 3883 for $[Fe(sal)_2trien]NO_3·H_2O$, of which 2560, 1186, 2614, and 2468, respectively, had $F_o^2 > 3\sigma(F_o^2)$, where $\sigma(F_o^2)$ was estimated from counting statistics.[28] These data were used in the final refinement of the structural parameters.

Results and Discussion

Spin State Characterization of the Compounds. At room temperature the $[Fe(acac)_2trien]PF_6$ and $[Fe(acacCl)_2trien]PF_6$ compounds of interest are $S = 5/2$ high-spin species in the solid state with μ_{eff} being ~6.0 μ_B. On the other hand, the $[Fe(sal)_2trien]X$ (X = $Cl^-·2H_2O$ and $NO_3^-·H_2O$) derivatives are essentially $S = ½$ low-spin species with $\mu_{eff}(Cl^-) = 1.94$ μ_B and $\mu_{eff}(NO_3^-) = 2.47$ μ_B.[16] Figure 2 depicts variable-temperature magnetic data for several different deriva-

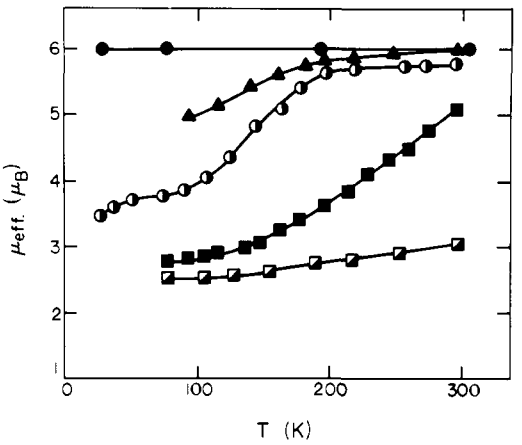

Figure 2. μ_{eff} vs. temperature data for the iron(III) complexes in the solid state: ●, $[Fe(acac)_2trien]PF_6$; ▲, $[Fe(acacCl)_2trien]PF_6$; ◐, $[Fe(sal)_2trien]PF_6$; ■, $[Fe(sal)_2trien]BPh_4$; ◪, $[Fe(acac)_2trien]BPh_4$.

Table II. Variable-Temperature Mössbauer Data for the Variable-Spin Iron Complexes

Compd	Temp, K	δ, mm s^{-1} [a-c]	ΔE_Q, mm s^{-1} [d]
$[Fe(acac)_2trien]PF_6$	298	0.68 (hs)	
$[Fe(acac)_2trien]BPh_4$	298	0.68 (hs)	
		0.47 (ls)	2.23
	120	0.47 (ls)	2.23
$[Fe(acacCl)_2trien]PF_6$	298	0.56 (hs)	
$[Fe(sal)_2trien]PF_6$	298	0.55 (hs)	
	113	0.64 (hs)	
		0.49 (ls)	2.97
$[Fe(sal)_2trien]BPh_4$	296	0.54 (hs)	
	235	0.54 (hs)	
		0.40 (ls)	2.45
	120	0.40 (ls)	2.45
$[Fe(sal)_2trien]Cl\cdot 2H_2O$	298	0.45 (ls)	2.56
$[Fe(sal)_2trien]NO_3\cdot H_2O$	296	0.44 (ls)	2.58

[a] Spin state of the iron center indicated in parentheses as either low-spin (ls) or high-spin (hs). [b] Measured relative to midpoint of room temperature sodium nitroprusside (SNP) spectrum. [c] Maximum standard deviation: 0.03 mm s^{-1}. [d] Maximum standard deviation: 0.06 mm s^{-1}.

tives of the $[Fe(acac)_2trien]^+$ and $[Fe(sal)_2trien]^+$ families, indicating anomalous magnetic behavior characteristic of a $^2T_2 \rightleftarrows {}^6A_1$ spin-equilibrium process as also found in the solution state.[16,17] Only the $[Fe(acac)_2trien]PF_6$ compound appears to remain fully high spin, even down to 20 K. The actual μ_{eff} vs. temperature data are in Table I.[29]

Variable-temperature Mössbauer spectral data, as reported in Table II, also serve to characterize the anomalous magnetic properties as arising from spin state equilibria. At temperatures where $\mu_{eff} \sim 5.9$-$6.0\ \mu_B$, the spectra are singlets and typical of those for $S = {}^5/_2$ iron(III) centers with δ(SNP) ranging from 0.54 to 0.64 mm s^{-1}. At lower temperatures where μ_{eff} approaches the $S = {}^1/_2$ low-spin value of $\sim 2.0\ \mu_B$, the spectra have large quadrupole split doublets (2.2-3.0 mm s^{-1}) with more negative δ shift values ranging from 0.44 to 0.47 mm s^{-1}. Such large quadrupole splittings for the $S = {}^1/_2$ spin isomer are somewhat unusual, but understandable in view of the significant tetragonal distortion as revealed by the crystal structure determinations for the $S = {}^1/_2$ compound to be discussed below. Typical high-spin and low-spin Mössbauer spectra are shown in Figures 3a and 3c for the $[Fe(acac)_2trien]PF_6$ (298 K) and $[Fe(acac)_2trien]BPh_4$ (120 K) compounds, respectively. For those temperatures where μ_{eff} is of an intermediate value, the

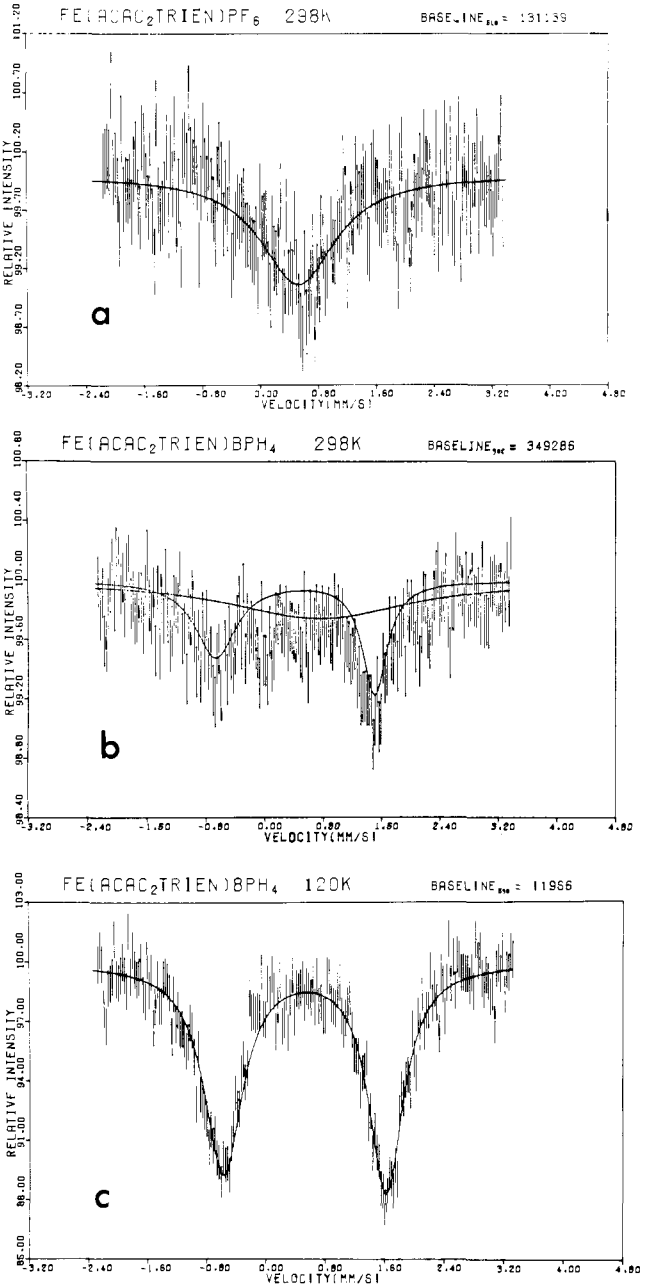

Figure 3. Mössbauer spectrum of (a) $[Fe(acac)_2trien]PF_6$ at 298 K, (b) $[Fe(acac)_2trien]BPh_4$ at 298 K, and (c) $[Fe(acac)_2trien]BPh_4$ at 120 K.

Mössbauer spectrum consists of a superimposition of both high- and low-spin signals as shown in Figure 3b for the $[Fe(acac)_2trien]BPh_4$ compound at 298 K. This spectral feature is typical of all the "intermediate moment" spectra for these compounds, and indicates that the lifetimes of the $S = {}^1/_2$ and $S = {}^5/_2$ spin states in the solid are $\gtrsim 10^{-7}$ s, i.e., the Mössbauer transition time scale. Although a great increase in the collection times ($\sim$12 h) would have improved the signal to noise ratio, the Mössbauer spectra are good enough to detect the $S = {}^1/_2$ and $S = {}^5/_2$ spin states and to place an upper limit of 10^{-7} s on the spin state lifetimes. In solution the lifetimes have been directly measured by laser Raman temperature-jump kinetics[16,17,23b] and, in general, determined to be about the same or shorter than Mössbauer spectroscopy indicates them to be in the solid state.

Determination, Refinement, and Discussion of the Structures. $[Fe(acacCl)_2trien]PF_6$. The positions of the iron, the chlorine, and four of the ligand atoms were determined from a three-

Table III. Positional and Thermal Parameters and Their Estimated Standard Deviations[a]

Atom	*X*	*Y*	*Z*	*B*(1,1)	*B*(2,2)	*B*(3,3)	*B*(1,2)	*B*(1,3)	*B*(2,3)
				A. $[Fe(acac)_2trien]PF_6$					
Fe	0.097 21 (3)	0.210 76 (6)	0.129 23 (5)	0.001 95 (1)	0.005 62 (5)	0.004 32 (3)	−0.000 28 (5)	0.003 36 (3)	−0.000 16 (7)
P1	0.217 26 (7)	0.4643 (1)	0.5588 (1)	0.002 50 (3)	0.0069 (1)	0.006 19 (7)	0.0004 (1)	0.004 00 (7)	0.0008 (2)
F1	0.2319 (3)	0.5775 (4)	0.5574 (4)	0.0100 (2)	0.0097 (4)	0.0187 (4)	−0.0054 (4)	0.0182 (3)	−0.0054 (6)
F2	0.1981 (3)	0.3528 (4)	0.5519 (4)	0.0102 (2)	0.0095 (4)	0.0180 (4)	−0.0047 (4)	0.0168 (4)	−0.0030 (6)
F3	0.2773 (3)	0.4121 (8)	0.6023 (5)	0.0029 (1)	0.0258 (10)	0.0072 (4)	0.0107 (6)	0.0033 (4)	0.0005 (11)
F4	0.2211 (5)	0.4559 (7)	0.4606 (5)	0.0105 (4)	0.0126 (7)	0.0033 (3)	−0.0049 (9)	0.0068 (5)	−0.0008 (8)
F5	0.1565 (4)	0.5195 (8)	0.5274 (7)	0.0039 (2)	0.0188 (8)	0.0177 (7)	0.0112 (6)	0.0091 (5)	0.0216 (11)
F6	0.2153 (6)	0.4685 (8)	0.6622 (6)	0.0127 (4)	0.0161 (8)	0.0082 (5)	0.0154 (9)	0.0125 (6)	0.0085 (10)
F3′	0.2804 (4)	0.4656 (13)	0.6356 (6)	0.0023 (2)	0.0470 (20)	0.0080 (5)	−0.0051 (10)	0.0011 (5)	0.0146 (16)
F4′	0.2408 (4)	0.4644 (9)	0.4784 (6)	0.0112 (2)	0.0190 (11)	0.0244 (5)	−0.0035 (9)	0.0305 (4)	−0.0020 (13)
F5′	0.1530 (4)	0.4598 (8)	0.4768 (6)	0.0041 (2)	0.0220 (10)	0.0082 (5)	−0.0085 (8)	0.0028 (5)	−0.0042 (13)
F6′	0.1961 (3)	0.4715 (7)	0.6404 (5)	0.0057 (1)	0.0150 (7)	0.0162 (3)	−0.0085 (5)	0.0179 (3)	−0.0143 (8)
O1	0.0710 (2)	0.0733 (3)	0.1052 (2)	0.002 95 (8)	0.0061 (2)	0.0045 (2)	−0.0016 (2)	0.0042 (2)	−0.0009 (3)
O2	0.0248 (2)	0.2836 (3)	0.0555 (2)	0.002 15 (7)	0.0079 (3)	0.0054 (2)	0.0012 (2)	0.0036 (2)	0.0018 (4)
N1	0.0843 (2)	0.2022 (3)	0.2574 (3)	0.002 17 (8)	0.0062 (3)	0.0045 (2)	−0.0001 (3)	0.0033 (2)	−0.0015 (4)
N2	0.1394 (2)	0.3475 (3)	0.2048 (3)	0.002 95 (11)	0.0057 (3)	0.0056 (2)	−0.0014 (3)	0.0032 (2)	0.0004 (5)
N3	0.1904 (2)	0.1669 (4)	0.1897 (3)	0.002 05 (9)	0.0069 (3)	0.0055 (2)	0.0003 (3)	0.0032 (2)	0.0009 (5)
N4	0.1203 (2)	0.2218 (3)	0.0107 (3)	0.002 13 (8)	0.0065 (3)	0.0051 (2)	0.0000 (3)	0.0036 (2)	0.0003 (4)
C1	0.0678 (2)	0.0042 (4)	0.1642 (4)	0.002 17 (10)	0.0061 (4)	0.0050 (2)	−0.0006 (3)	0.0032 (2)	0.0001 (5)
C2	0.0726 (2)	0.0213 (4)	0.2554 (4)	0.002 01 (10)	0.0070 (4)	0.0049 (2)	−0.0000 (4)	0.0030 (2)	−0.0003 (6)
C3	0.0798 (2)	0.1182 (5)	0.2999 (3)	0.001 52 (9)	0.0084 (4)	0.0043 (2)	0.0003 (3)	0.0030 (2)	0.0004 (5)
C4	0.0919 (3)	0.2967 (5)	0.3114 (4)	0.003 46 (14)	0.0075 (4)	0.0065 (3)	−0.0002 (4)	0.0054 (3)	−0.0034 (6)
C5	0.1007 (3)	0.3831 (5)	0.2519 (4)	0.003 80 (16)	0.0067 (4)	0.0073 (3)	0.0000 (5)	0.0044 (4)	−0.0041 (6)
C6	0.2018 (3)	0.3261 (5)	0.2712 (5)	0.002 88 (15)	0.0076 (4)	0.0073 (4)	−0.0032 (4)	0.0026 (4)	−0.0016 (7)
C7	0.2286 (3)	0.2563 (5)	0.2209 (4)	0.002 07 (12)	0.0096 (5)	0.0064 (3)	−0.0006 (4)	0.0021 (3)	0.0022 (7)
C8	0.1989 (3)	0.1105 (5)	0.1126 (5)	0.002 33 (11)	0.0093 (5)	0.0089 (4)	0.0030 (4)	0.0050 (3)	0.0023 (7)
C9	0.1759 (2)	0.1710 (5)	0.0193 (4)	0.002 47 (11)	0.0096 (5)	0.0066 (3)	0.0015 (4)	0.0050 (3)	−0.0000 (7)
C10	0.0929 (2)	0.2780 (4)	−0.0665 (4)	0.002 67 (11)	0.0069 (4)	0.0045 (2)	−0.0030 (4)	0.0035 (2)	−0.0015 (5)
C11	0.0382 (2)	0.3320 (5)	−0.0848 (4)	0.002 30 (12)	0.0065 (4)	0.0063 (3)	−0.0005 (4)	0.0030 (3)	0.0006 (6)
C12	0.0077 (2)	0.3290 (4)	−0.0257 (4)	0.002 25 (12)	0.0053 (3)	0.0071 (3)	−0.0006 (4)	0.0029 (3)	−0.0005 (6)
C1M	0.0558 (3)	−0.1011 (5)	0.1224 (5)	0.005 22 (20)	0.0056 (4)	0.0067 (3)	−0.0027 (5)	0.0052 (4)	−0.0020 (6)
C3M	0.0827 (3)	0.1206 (5)	0.4019 (4)	0.003 25 (12)	0.0105 (5)	0.0042 (2)	−0.0002 (4)	0.0050 (2)	0.0004 (6)
C10M	0.1177 (3)	0.2903 (6)	−0.1429 (4)	0.003 95 (14)	0.0117 (6)	0.0056 (3)	−0.0020 (5)	0.0065 (3)	0.0008 (7)
C12M	−0.5020 (3)	0.3838 (5)	−0.0547 (5)	0.002 37 (13)	0.0091 (5)	0.0102 (4)	0.0038 (4)	0.0037 (4)	0.0038 (8)
H41	0.129 (2)	0.292 (3)	0.372 (3)	4. (1)					
H42	0.057 (2)	0.312 (4)	0.325 (4)	8. (1)					
H51	0.116 (2)	0.449 (4)	0.288 (3)	7. (1)					
H52	0.063 (2)	0.403 (4)	0.187 (3)	6. (1)					
H61	0.218 (2)	0.376 (4)	0.291 (3)	7. (1)					
H62	0.192 (2)	0.276 (4)	0.332 (4)	9. (2)					
H71	0.267 (2)	0.234 (3)	0.268 (3)	5. (1)					
H72	0.217 (2)	0.304 (3)	0.157 (3)	6. (1)					
H81	0.228 (2)	0.091 (4)	0.128 (3)	7. (1)					
H82	0.169 (2)	0.048 (3)	0.101 (3)	6. (1)					
H91	0.165 (2)	0.119 (3)	−0.031 (3)	5. (1)					
H92	0.206 (2)	0.224 (3)	0.021 (3)	4. (1)					
HN2	0.136 (2)	0.386 (3)	0.163 (3)	4. (1)					

B. $[Fe(acacCl)_2trien]PF_6$

Fe	0.102 44 (9)	0.2175 (2)	0.1405 (1)	0.001 97 (4)	0.0057 (1)	0.0065 (1)	0.0008 (2)	0.0035 (1)	0.0007 (3)
Cl(1)	0.0764 (2)	−0.0769 (4)	0.3212 (4)	0.0053 (2)	0.0130 (4)	0.0147 (4)	0.0017 (5)	0.0063 (4)	0.0145 (7)
Cl2	0.0159 (3)	0.4131 (6)	−0.1482 (4)	0.0073 (2)	0.0319 (8)	0.0170 (4)	0.0129 (7)	0.0098 (5)	0.0273 (10)
P1	0.2222 (2)	0.4564 (3)	0.5675 (3)	0.0023 (1)	0.0065 (3)	0.0089 (3)	−0.0008 (3)	0.0029 (3)	0.0020 (5)
F1	0.2416 (6)	0.563 (1)	0.565 (1)	0.0084 (4)	0.013 (1)	0.0235 (11)	−0.005 (1)	0.0149 (10)	−0.003 (2)
F2	0.1993 (7)	0.354 (1)	0.566 (1)	0.0070 (5)	0.014 (1)	0.0330 (19)	−0.003 (1)	0.0090 (15)	0.008 (3)
F3	0.2745 (7)	0.387 (2)	0.597 (1)	0.0032 (4)	0.021 (2)	0.0124 (14)	0.016 (1)	0.0034 (11)	0.002 (3)
F4	0.2120 (14)	0.450 (2)	0.468 (1)	0.0129 (12)	0.013 (2)	0.0064 (10)	−0.000 (3)	0.0094 (16)	−0.001 (3)
F5	0.1644 (6)	0.521 (1)	0.555 (1)	0.0018 (3)	0.010 (1)	0.0134 (13)	0.008 (1)	0.0035 (11)	0.008 (2)
F6	0.2391 (12)	0.476 (2)	0.676 (1)	0.0101 (10)	0.013 (2)	0.0048 (11)	0.011 (2)	−0.0010 (18)	−0.001 (3)
F3′	0.2822 (8)	0.444 (2)	0.637 (2)	0.0015 (4)	0.046 (4)	0.0146 (15)	−0.008 (2)	−0.0024 (13)	0.034 (3)
F4′	0.2547 (11)	0.462 (2)	0.498 (2)	0.0076 (5)	0.023 (3)	0.0212 (15)	−0.007 (2)	0.0196 (11)	−0.004 (4)
F5′	0.1664 (9)	0.447 (2)	0.487 (1)	0.0045 (6)	0.030 (3)	0.0077 (13)	−0.015 (2)	−0.0013 (15)	0.002 (4)
F6′	0.1958 (8)	0.455 (2)	0.636 (1)	0.0041 (5)	0.027 (3)	0.0071 (9)	−0.004 (2)	0.0073 (9)	−0.012 (3)
O1	0.0769 (4)	0.0818 (7)	0.1181 (6)	0.0029 (2)	0.0056 (7)	0.0086 (6)	−0.0013 (7)	0.0054 (5)	0.001 (1)
O2	0.0300 (4)	0.2833 (8)	0.0720 (6)	0.0020 (2)	0.0112 (9)	0.0076 (6)	0.0023 (8)	0.0030 (5)	0.004 (1)
N1	0.0859 (4)	0.2023 (8)	0.2602 (7)	0.0022 (3)	0.0057 (9)	0.0077 (7)	0.0008 (9)	0.0038 (6)	−0.003 (1)
N2	0.1419 (5)	0.3545 (8)	0.2106 (7)	0.0036 (3)	0.0051 (9)	0.0066 (7)	−0.0007 (10)	0.0036 (7)	0.001 (1)
N3	0.1959 (5)	0.1778 (8)	0.1956 (7)	0.0022 (3)	0.0068 (9)	0.0058 (7)	0.0007 (9)	0.0016 (7)	−0.001 (1)
N4	0.1270 (4)	0.2362 (8)	0.0290 (7)	0.0015 (2)	0.0044 (8)	0.0079 (7)	0.0003 (8)	0.0024 (6)	−0.000 (1)
C1	0.0746 (6)	0.010 (1)	0.1736 (9)	5.3 (4)					
C2	0.0773 (6)	0.028 (1)	0.2559 (9)	4.6 (4)					
C3	0.0814 (6)	0.119 (1)	0.3006 (9)	5.1 (4)					
C4	0.0895 (7)	0.298 (1)	0.3080 (10)	7.2 (5)					
C5	0.1007 (7)	0.383 (1)	0.2549 (11)	7.4 (5)					
C6	0.2037 (6)	0.334 (1)	0.2743 (10)	6.3 (4)					
C7	0.2321 (7)	0.267 (1)	0.2288 (10)	6.6 (4)					
C8	0.2051 (6)	0.128 (1)	0.1216 (10)	6.1 (4)					
C9	0.1838 (6)	0.188 (1)	0.0376 (10)	6.0 (4)					
C10	0.1010 (6)	0.292 (1)	−0.0444 (9)	4.8 (3)					
C11	0.0447 (6)	0.337 (1)	−0.0567 (9)	5.7 (4)					
C12	0.0129 (6)	0.329 (1)	−0.0053 (9)	5.7 (4)					
C1M	0.0655 (7)	−0.094 (1)	0.1241 (11)	8.3 (5)					
C3M	0.0776 (7)	0.124 (1)	0.3972 (10)	6.8 (4)					
C10M	0.1295 (7)	0.308 (1)	−0.1159 (10)	6.3 (4)					
C12M	−0.0504 (7)	0.379 (1)	−0.0321 (11)	7.6 (5)					
H41	0.1209 (0)	0.2979 (0)	0.3684 (0)	5.0000 (0)					
H42	0.0525 (0)	0.3103 (0)	0.3209 (0)	5.0000 (0)					
H51	0.1157 (0)	0.4426 (0)	0.2942 (0)	5.0000 (0)					
H52	0.0618 (0)	0.4069 (0)	0.2115 (0)	5.0000 (0)					
H61	0.2272 (0)	0.3966 (0)	0.2889 (0)	5.0000 (0)					
H62	0.2057 (0)	0.3045 (0)	0.3275 (0)	5.0000 (0)					
H71	0.2711 (0)	0.2447 (0)	0.2769 (0)	5.0000 (0)					
H72	0.2432 (0)	0.2981 (0)	0.1848 (0)	5.0000 (0)					
H81	0.2455 (0)	0.1053 (0)	0.1344 (0)	5.0000 (0)					
H82	0.1814 (0)	0.0633 (0)	0.1077 (0)	5.0000 (0)					
H91	0.1787 (0)	0.1471 (0)	−0.0163 (0)	5.0000 (0)					
H92	0.2136 (0)	0.2368 (0)	0.0400 (0)	5.0000 (0)					
HN2	0.1437 (0)	0.4086 (0)	0.1716 (0)	5.0000 (0)					
HN3	0.2102 (0)	0.1373 (0)	0.2493 (0)	5.0000 (0)					

Table III (*Continued*)

Atom	*X*	*Y*	*Z*	*B*(1,1)	*B*(2,2)	*B*(3,3)	*B*(1,2)	*B*(1,3)	*B*(2,3)
				C. [Fe(sal)$_2$trien]Cl·2H$_2$O					
Fe	−0.223 35 (2)	0.040 46 (4)	0.074 90 (3)	0.001 84 (1)	0.004 28 (4)	0.003 91 (3)	0.000 53 (4)	0.000 54 (3)	−0.000 20 (6)
Cl	−0.098 01 (5)	−0.5738 (1)	0.122 20 (9)	0.003 57 (3)	0.0093 (1)	0.009 61 (8)	−0.0002 (1)	0.001 22 (9)	−0.0030 (2)
OA	−0.2712 (1)	0.1757 (2)	−0.0243 (2)	0.002 40 (6)	0.0067 (2)	0.0041 (1)	0.0025 (2)	0.0015 (2)	0.0015 (3)
OB	−0.3121 (1)	−0.0421 (2)	0.0863 (2)	0.002 31 (6)	0.0068 (2)	0.0051 (1)	−0.0015 (2)	0.0010 (2)	−0.0004 (3)
OC	−0.2201 (2)	−0.3538 (3)	0.0958 (3)	0.004 33 (10)	0.0080 (3)	0.0158 (3)	0.0003 (3)	0.0013 (3)	−0.0010 (5)
OD	0.0184 (2)	−0.6794 (3)	−0.0232 (3)	0.005 39 (11)	0.0091 (3)	0.0173 (3)	−0.0003 (3)	0.0085 (3)	−0.0038 (6)
N1	−0.2262 (1)	0.1411 (2)	0.2101 (2)	0.002 12 (7)	0.0052 (3)	0.0037 (2)	−0.0002 (2)	0.0005 (2)	−0.0000 (4)
N2	−0.1665 (1)	−0.0916 (3)	0.1858 (2)	0.002 89 (9)	0.0048 (3)	0.0059 (2)	0.0010 (3)	−0.0005 (2)	0.0001 (4)
N3	−0.1233 (1)	0.1092 (3)	0.0661 (2)	0.002 07 (8)	0.0049 (3)	0.0073 (2)	0.0002 (3)	0.0015 (2)	−0.0011 (4)
N4	−0.2168 (1)	−0.0594 (2)	−0.0594 (2)	0.002 47 (8)	0.0037 (2)	0.0045 (2)	0.0010 (2)	0.0007 (2)	−0.0009 (4)
C1	−0.3095 (2)	0.3122 (3)	0.1160 (2)	0.001 82 (9)	0.0046 (3)	0.0055 (2)	−0.0003 (3)	0.0015 (2)	−0.0008 (5)
C2	−0.3118 (2)	0.2730 (3)	0.0032 (2)	0.001 84 (8)	0.0050 (3)	0.0053 (2)	0.0004 (3)	0.0015 (2)	0.0015 (5)
C3	−0.3597 (2)	0.3433 (4)	−0.0846 (3)	0.002 63 (10)	0.0091 (4)	0.0057 (2)	0.0029 (3)	0.0015 (3)	0.0026 (5)
C4	−0.4013 (2)	0.4482 (4)	−0.0618 (3)	0.002 99 (12)	0.0088 (4)	0.0085 (3)	0.0041 (4)	0.0010 (3)	0.0050 (6)
C5	−0.3984 (2)	0.4879 (4)	0.0483 (3)	0.002 78 (11)	0.0061 (4)	0.0108 (3)	0.0030 (3)	0.0019 (3)	−0.0014 (6)
C6	−0.3537 (2)	0.4205 (3)	0.1360 (3)	0.002 57 (10)	0.0059 (3)	0.0076 (3)	0.0002 (3)	0.0022 (3)	−0.0033 (5)
C7	−0.2638 (2)	0.2476 (3)	0.2134 (2)	0.002 12 (9)	0.0057 (3)	0.0045 (2)	−0.0008 (3)	0.0015 (2)	−0.0014 (5)
C8	−0.1850 (2)	0.0814 (3)	0.3177 (3)	0.002 89 (11)	0.0080 (4)	0.0040 (2)	0.0011 (4)	0.0002 (3)	0.0003 (5)
C9	−0.1859 (2)	−0.0672 (4)	0.2970 (3)	0.003 47 (12)	0.0075 (4)	0.0052 (2)	0.0012 (4)	0.0004 (3)	0.0033 (5)
C10	−0.0865 (2)	−0.0869 (4)	0.1886 (3)	0.002 94 (12)	0.0106 (4)	0.0070 (3)	0.0046 (4)	−0.0009 (3)	0.0001 (6)
C11	−0.0650 (2)	0.0516 (4)	0.1600 (3)	0.001 74 (10)	0.0134 (5)	0.0076 (3)	0.0008 (4)	0.0002 (3)	−0.0022 (6)
C12	−0.1134 (2)	0.0842 (4)	−0.0506 (3)	0.002 50 (10)	0.0085 (4)	0.0067 (2)	0.0008 (3)	0.0031 (3)	0.0011 (5)
C13	−0.1454 (2)	−0.0509 (4)	−0.0916 (3)	0.003 09 (11)	0.0089 (4)	0.0059 (2)	0.0019 (4)	0.0029 (3)	−0.0015 (5)
C1B	−0.3424 (2)	−0.1396 (3)	−0.1017 (3)	0.002 61 (10)	0.0048 (3)	0.0055 (2)	−0.0005 (3)	−0.007 (3)	0.0009 (5)
C2B	−0.3596 (2)	−0.0987 (3)	0.0009 (3)	0.002 28 (10)	0.0042 (3)	0.0062 (2)	0.0000 (3)	0.0000 (3)	0.0031 (5)
C3B	−0.4311 (2)	−0.1242 (3)	0.0158 (3)	0.002 37 (10)	0.0068 (4)	0.0090 (3)	0.0001 (3)	0.0011 (3)	0.0031 (6)
C4B	−0.4838 (2)	−0.1844 (4)	−0.0696 (4)	0.002 34 (11)	0.0081 (4)	0.0130 (4)	−0.0014 (4)	−0.0003 (4)	0.0031 (7)
C5B	−0.4671 (2)	−0.2234 (4)	−0.1702 (4)	0.003 57 (13)	0.0083 (4)	0.0104 (4)	−0.0026 (4)	−0.0042 (4)	0.0014 (7)
C6B	−0.3976 (2)	−0.2027 (4)	−0.1863 (3)	0.003 82 (13)	0.0070 (4)	0.0068 (3)	−0.0015 (4)	−0.0014 (3)	−0.0005 (6)
C7B	−0.2709 (2)	−0.1220 (3)	−0.1246 (3)	0.003 40 (11)	0.0041 (3)	0.0047 (2)	0.0013 (3)	0.0008 (3)	−0.0010 (5)
H3	−0.362 (2)	0.318 (4)	−0.162 (3)	4.3 (8)					
H4	−0.430 (2)	0.490 (4)	−0.121 (3)	5.1 (9)					
H5	−0.426 (2)	0.548 (4)	0.066 (3)	4.6 (9)					
H6	−0.354 (2)	0.442 (3)	0.209 (3)	3.4 (8)					
H7	−0.262 (2)	0.285 (3)	0.286 (2)	2.7 (7)					
H181	−0.135 (2)	0.119 (3)	0.333 (2)	2.7 (7)					
H182	−0.211 (2)	0.103 (3)	0.383 (3)	3.4 (7)					
H191	−0.232 (2)	−0.108 (3)	0.285 (3)	3.3 (7)					
H192	−0.152 (2)	−0.115 (4)	0.357 (3)	4.8 (9)					
H201	−0.078 (2)	−0.143 (4)	0.134 (3)	4.7 (9)					
H202	−0.059 (2)	−0.113 (4)	0.261 (3)	4.1 (8)					
H211	−0.019 (2)	0.057 (4)	0.139 (3)	5.3 (10)					
H212	−0.059 (2)	0.118 (4)	0.226 (3)	4.6 (8)					
H221	−0.061 (2)	0.087 (4)	−0.045 (3)	4.3 (8)					
H222	−0.139 (2)	0.152 (3)	−0.095 (3)	3.1 (7)					
H231	−0.151 (2)	−0.057 (3)	−0.171 (3)	3.9 (8)					
H232	−0.112 (2)	−0.122 (4)	−0.053 (3)	4.4 (8)					
H7B	−0.262 (2)	−0.159 (3)	−0.194 (3)	3.5 (8)					
H6B	−0.383 (2)	−0.225 (4)	−0.253 (3)	4.5 (8)					

H5B	−0.500 (2)	−0.260 (5)	−0.229 (3)	7.0 (11)
H4B	−0.531 (2)	−0.199 (4)	−0.056 (3)	5.3 (9)
H3B	−0.442 (2)	−0.095 (3)	0.078 (3)	2.9 (7)
HN2	−0.185 (2)	−0.164 (3)	0.161 (3)	3.5 (8)
HN3	−0.124 (2)	0.192 (4)	0.076 (3)	4.3 (8)
HC1	−0.175 (2)	−0.419 (4)	0.094 (3)	7.7 (11)
HC2	−0.258 (2)	−0.381 (4)	0.067 (3)	7.0 (10)
HD1	−0.014 (2)	−0.648 (4)	0.020 (3)	5.5 (9)
HD2	0.044 (2)	−0.626 (4)	−0.044 (3)	6.3 (10)

D. $[Fe(sal)_2trien]NO_3 \cdot H_2O$

Fe	0.092 95 (5)	0.031 68 (6)	−0.223 97 (3)	0.004 69 (4)	0.006 73 (5)	0.001 96 (2)	0.0000 (1)	0.001 55 (4)	−0.000 37 (7)
OA	0.1627 (2)	0.1712 (3)	−0.2704 (1)	0.0036 (2)	0.0089 (3)	0.002 18 (9)	0.0001 (4)	0.0002 (2)	0.0024 (3)
OB	0.0286 (2)	−0.0472 (3)	−0.3122 (1)	0.0050 (2)	0.0103 (4)	0.002 40 (9)	−0.0004 (5)	0.0013 (2)	−0.0023 (3)
OC	0.0798 (3)	−0.3629 (4)	−0.2256 (2)	0.0142 (4)	0.0105 (4)	0.004 49 (14)	0.0002 (7)	0.0026 (4)	0.0005 (4)
OD	0.0927 (4)	0.3860 (4)	0.8633 (2)	0.0167 (5)	0.0148 (5)	0.004 43 (15)	0.0054 (9)	−0.0043 (4)	−0.0065 (5)
OE	0.1692 (6)	0.5476 (6)	0.9236 (3)	0.0146 (7)	0.0116 (8)	0.004 44 (24)	0.0016 (13)	−0.0005 (7)	−0.0016 (8)
OF	0.1656 (7)	0.3531 (8)	0.9729 (4)	0.0172 (9)	0.0132 (10)	0.004 15 (28)	0.0110 (16)	−0.0044 (9)	−0.0014 (9)
OG	0.1024 (11)	0.5528 (9)	0.9351 (6)	0.0249 (15)	0.0099 (11)	0.004 73 (39)	0.0141 (21)	−0.0039 (13)	−0.0055 (11)
OH	0.2085 (10)	0.3516 (13)	0.9654 (7)	0.0106 (11)	0.0137 (16)	0.004 73 (47)	0.0017 (23)	−0.0024 (12)	−0.0063 (14)
OI	0.1044 (23)	0.3564 (23)	0.9746 (12)	0.0229 (30)	0.0193 (32)	0.003 70 (76)	0.0057 (53)	0.0019 (24)	−0.0015 (27)
N1	−0.0454 (3)	0.1313 (3)	−0.2251 (2)	0.0046 (2)	0.0079 (4)	0.0027 (1)	−0.0003 (6)	0.0024 (3)	−0.0018 (4)
N2	0.0162 (3)	−0.1057 (4)	−0.1695 (2)	0.0083 (3)	0.0072 (4)	0.0027 (1)	−0.0011 (6)	0.0034 (3)	−0.0010 (4)
N3	0.1606 (3)	0.0958 (4)	−0.1247 (2)	0.0080 (3)	0.0065 (4)	0.0022 (1)	0.0002 (6)	0.0016 (3)	−0.0011 (4)
N	0.1340 (5)	0.4279 (4)	0.9219 (2)	0.0177 (6)	0.0105 (6)	0.0034 (2)	0.0023 (9)	−0.0031 (5)	−0.0042 (5)
N4	0.2340 (3)	−0.0644 (3)	−0.2199 (2)	0.0036 (2)	0.0035 (4)	0.0010 (1)	0.0018 (5)	0.0008 (3)	0.0005 (3)
C1	−0.0046 (3)	0.3034 (4)	−0.3087 (2)	0.0050 (3)	0.0068 (5)	0.0020 (1)	0.0009 (7)	−0.003 (3)	−0.0013 (4)
C2	0.1083 (3)	0.2673 (4)	−0.3113 (2)	0.0053 (3)	0.0076 (5)	0.0015 (1)	−0.0007 (7)	−0.0004 (3)	−0.0003 (4)
C3	0.1667 (4)	0.3402 (5)	−0.3590 (3)	0.0063 (4)	0.0100 (6)	0.0028 (2)	−0.0003 (8)	0.0002 (4)	0.0020 (5)
C4	0.1171 (4)	0.4440 (5)	−0.4005 (3)	0.0099 (4)	0.0098 (6)	0.0027 (2)	−0.0016 (9)	0.0005 (4)	0.0027 (5)
C5	0.0058 (4)	0.4789 (5)	−0.3981 (3)	0.0110 (5)	0.0079 (5)	0.0029 (2)	0.0051 (9)	−0.0007 (5)	0.0017 (5)
C6	−0.0531 (4)	0.4098 (5)	−0.3526 (3)	0.0067 (4)	0.0098 (5)	0.0031 (2)	0.0042 (8)	−0.0005 (4)	−0.0025 (5)
C7	−0.0734 (3)	0.2364 (4)	−0.2623 (2)	0.0040 (3)	0.0086 (5)	0.0026 (1)	0.0018 (7)	0.0004 (3)	−0.0031 (4)
C8	−0.1258 (4)	0.0704 (5)	−0.1810 (3)	0.0054 (3)	0.0112 (6)	0.0043 (2)	−0.0011 (7)	0.0052 (4)	−0.0007 (6)
C9	−0.1068 (4)	−0.0797 (5)	−0.1829 (3)	0.0074 (4)	0.0099 (6)	0.0054 (2)	−0.0045 (8)	0.0063 (4)	−0.0015 (6)
C10	0.0669 (4)	−0.1098 (5)	−0.0911 (3)	0.0121 (5)	0.0113 (6)	0.0028 (1)	0.0003 (10)	0.0053 (4)	0.0028 (5)
C11	0.1067 (4)	0.0271 (6)	−0.0667 (2)	0.0103 (4)	0.0150 (7)	0.0019 (1)	0.0002 (10)	0.0033 (4)	−0.0013 (6)
C12	0.2854 (4)	0.0793 (5)	−0.1173 (2)	0.0074 (4)	0.0112 (6)	0.0021 (1)	−0.0024 (8)	−0.0015 (4)	−0.0003 (5)
C13	0.3099 (4)	−0.0533 (5)	−0.1517 (3)	0.0074 (4)	0.0117 (6)	0.0027 (2)	0.0049 (8)	0.0012 (4)	0.0026 (5)
C1B	0.1992 (4)	−0.1425 (4)	−0.3450 (2)	0.0073 (3)	0.0058 (5)	0.0024 (1)	−0.0003 (7)	0.0028 (4)	−0.0006 (4)
C2B	0.0841 (4)	−0.1032 (4)	−0.3607 (2)	0.0075 (3)	0.0058 (4)	0.0020 (1)	−0.0023 (7)	0.0021 (3)	−0.0002 (4)
C3B	0.0283 (4)	−0.1263 (5)	−0.4315 (3)	0.0086 (4)	0.0083 (5)	0.0026 (2)	−0.0031 (8)	0.0009 (4)	−0.0008 (5)
C4B	0.0804 (5)	−0.1849 (5)	−0.4843 (3)	0.0141 (6)	0.0113 (6)	0.0020 (2)	−0.0039 (10)	0.0021 (5)	−0.0013 (5)
C5B	0.1928 (5)	−0.2255 (5)	−0.4688 (3)	0.0139 (5)	0.0113 (6)	0.0031 (2)	−0.0029 (10)	0.0068 (4)	−0.0038 (5)
C6B	0.2490 (4)	−0.2048 (5)	−0.4007 (3)	0.0089 (4)	0.0101 (6)	0.0034 (2)	−0.0006 (9)	0.0043 (4)	−0.0016 (6)
C7B	0.2644 (3)	−0.1233 (4)	−0.2746 (2)	0.0050 (3)	0.0067 (5)	0.0034 (2)	0.0011 (7)	0.0015 (4)	0.0022 (5)
HN2	0.020 (3)	−0.187 (4)	−0.191 (2)	2.6 (9)					
H3	0.241 (4)	0.311 (5)	−0.362 (2)	4.3 (11)					
H4	0.154 (4)	0.499 (5)	−0.434 (3)	5.1 (12)					
H5	−0.024 (4)	0.556 (5)	−0.421 (2)	4.6 (12)					
H6	−0.124 (3)	0.434 (4)	−0.346 (2)	3.1 (10)					
H7	−0.140 (3)	0.275 (4)	−0.261 (2)	1.4 (8)					
H81	−0.200 (4)	0.084 (5)	−0.209 (2)	4.5 (12)					

Table III (*Continued*)

Atom	X	Y	Z	B(1,1)	Nitrate oxygen atom position	Occupancy	Probable nitrate positions	Estimated occupancy
H82	−0.107 (4)	0.105 (5)	−0.133 (3)	6.3 (14)	OD	1.0	(a) OD OE OF	0.4
H91	−0.136 (5)	−0.115 (6)	−0.230 (3)	8.2 (17)	OE	0.6	(b) OD OG OH	0.3
H92	−0.147 (3)	−0.124 (4)	−0.149 (2)	3.8 (10)	OF	0.5	(c) OD OE OI	0.2
H101	0.120 (4)	−0.164 (4)	−0.087 (2)	3.7 (11)	OG	0.4	(d) OD OF OG	0.1
H102	0.009 (4)	−0.137 (5)	−0.060 (3)	6.3 (14)	OH	0.3		
H111	0.156 (3)	0.024 (4)	−0.027 (2)	2.9 (9)	OI	0.2		
H112	0.049 (4)	0.091 (5)	−0.054 (2)	4.5 (11)				
H121	0.316 (4)	0.156 (4)	−0.147 (2)	3.9 (11)				
H122	0.328 (3)	0.085 (4)	−0.073 (2)	3.1 (10)				
H131	0.296 (3)	−0.124 (4)	−0.123 (2)	3.3 (10)				
H132	0.374 (4)	−0.061 (5)	−0.168 (3)	4.9 (12)				
HN3	0.152 (4)	0.192 (5)	−0.121 (3)	5.2 (13)				
H3B	−0.043 (4)	−0.098 (4)	−0.438 (2)	4.0 (11)				
H4B	0.038 (4)	−0.205 (5)	−0.528 (3)	6.4 (14)				
H5B	0.235 (4)	−0.273 (5)	−0.500 (3)	6.1 (14)				
H6B	0.312 (4)	−0.228 (5)	−0.391 (2)	4.2 (11)				
H7B	0.329 (3)	−0.157 (3)	−0.269 (2)	1.0 (7)				
HOC1	0.094 (4)	−0.422 (5)	−0.187 (3)	5.2 (12)				
HOC2	0.067 (5)	−0.402 (7)	−0.250 (4)	10.6 (19)				

[a] The form of the anisotropic thermal parameter is $\exp[-(B(1,1)*H*H + B(2,2)*K*K + B(3,3)*L*L + B(1,2)*H*K + B(1,3)*H*L + B(2,3)*K*L)]$.

dimensional Patterson synthesis. Full-matrix least-squares refinement was based on F, and the function minimized was $\Sigma w(|F_o| - |F_c|)^2$. The weights w were then taken as $[2F_o/\sigma(F_o^2)]^2$, where $|F_o|$ and $|F_c|$ are the observed and calculated structure factor amplitudes. The atomic scattering factors for nonhydrogen atoms were taken from Cromer and Waber,[30] and those for hydrogen from Stewart et al.[31] The effects of anomalous dispersion for all nonhydrogen atoms were included in F_c using the values of Cromer and Ibers[32] for $\Delta f'$ and $\Delta f''$. Agreement factors are defined as $R = \Sigma||F_o| - |F_c||/\Sigma|F_o|$ and $R_w = [\Sigma w(|F_o| - |F_c|)^2/\Sigma w|F_o|^2]^{1/2}$. The computing system and programs used have been described.[33] The intensity data were phased sufficiently well by the "heavy" atom positions determined from the Patterson function to permit location of the remaining nonhydrogen atoms by difference Fourier syntheses. The fluorine atoms of the PF_6^- ion exhibited positional disorder which was not clearly resolved. At this stage it was observed that better crystals could be obtained of $[Fe(acac)_2trien]PF_6$ than of $[Fe(acacCl)_2trien]PF_6$, so that the former compound might give similar but more accurate structural information. The two complexes were found to be isomorphous.

$[Fe(acac)_2trien]PF_6$. Using the atomic positional parameters for $[Fe(acacCl)_2trien]PF_6$ as starting values, least-squares refinement and Fourier syntheses were calculated to locate the disordered fluorine and the nonmethyl hydrogen atoms. The PF_6^- ion was found to be disordered in two main positions, related by a rotation of about 45° about the F-P-F axis, and having equal occupancy within experimental error.

Anisotropic temperature factors were introduced for all nonhydrogen atoms. The hydrogen atoms were included in the refinement for three cycles and subsequently held fixed. The model converged with $R = 5.4$, $R_w = 7.0\%$. The largest parameter shift at convergence was less than one-quarter of its estimated standard deviation. The error in an observation of unit weight is 2.5. Using the atomic parameters of the PF_6^- ion in $[Fe(acac)_2trien]PF_6$ as starting values in $[Fe(acacCl)_2trien]PF_6$, refinement was completed for the latter compound as above, except that the thermal parameters of the hydrogen atoms were held fixed at 5.0 Å^2. The model converged with $R = 6.7$, $R_w = 7.2\%$. The largest parameter shift at convergence was less than one-quarter of its estimated standard deviation. The error in an observation of unit weight is 3.3.

$[Fe(sal)_2trien]Cl\cdot 2H_2O$. The positions of the iron and four of the ligand atoms were determined from a three-dimensional Patterson synthesis, and the solution of the structure was completed as above. The chloride anion was found to be within hydrogen bonding distance of the two water oxygens, one of which is within hydrogen bonding distance of a ligand amine nitrogen; the existence of hydrogen bonding was confirmed by the location, from a Fourier synthesis of the hydrogen atoms involved (together with the other hydrogen atoms in the molecule). The model converged with $R = 3.4$, $R_w = 4.1\%$. The largest parameter shift at convergence was less than one-tenth of its estimated standard deviation. The error in an observation of unit weight is 2.1.

$[Fe(sal)_2trien]NO_3\cdot H_2O$. The iron and three of the ligand atoms were located from the Patterson synthesis, and the solution was completed as above. The nitrate anion was found to be disordered by rotation about one of the N-O bonds. This ion was also found to be within hydrogen bonding distance of a ligand amine nitrogen; hydrogen bonding was confirmed by the location of the hydrogen atoms from a Fourier synthesis. The model converged with $R = 4.5$, $R_w = 5.1\%$. The largest parameter shift at convergence was less than one-quarter of its estimated standard deviation. The error in an observation of unit weight is 2.1. A final difference Fourier synthesis was featureless for each complex. Tables of the observed structure

Table IV. Bond Distances (Å)

A. $[Fe(acac)_2]PF_6$ and $[Fe(acacCl)_2trien]PF_6$ (*A* and *B*, Respectively)

	A	*B*		*A*	*B*
Fe-O(1)	1.925 (3)	1.911 (6)	C(6)-C(7)	1.509 (6)	1.48 (1)
Fe-O(2)	1.935 (3)	1.905 (6)	C(8)-C(9)	1.530 (6)	1.48 (1)
Fe-N(1)	2.098 (3)	2.103 (8)	C(10)-C(11)	1.444 (6)	1.43 (1)
Fe-N(2)	2.181 (3)	2.179 (7)	C(10)-C(10M)	1.518 (6)	1.55 (1)
Fe-N(3)	2.168 (3)	2.167 (6)	C(11)-C(12)	1.379 (6)	1.32)1)
Fe-N(4)	2.098 (3)	2.089 (8)	C(12)-C(12M)	1.529 (7)	1.58 (1)
Cl(1)-C(2)		1.762 (9)	P(1)-F(1)	1.551 (3)	1.508 (3)
Cl(2)-C(11)		1.71 (1)	P(1)-F(2)	1.548 (3)	1.479 (3)
O(1)-C(1)	1.309 (5)	1.32 (1)	P(1)-F(3)	1.517 (8)	1.499 (3)
O(2)-C(12)	1.284 (5)	1.30 (1)	P(1)-F(4)	1.536 (8)	1.525 (3)
N(1)-C(3)	1.318 (5)	1.31 (1)	P(1)-F(5)	1.552 (5)	1.589 (3)
N(1)-C(4)	1.472 (6)	1.48 (1)	P(1)-F(6)	1.591 (9)	1.654 (3)
N(2)-C(5)	1.473 (6)	1.47 (1)	P(1)-F(3′)	1.518 (9)	1.477 (3)
N(2)-C(6)	1.481 (6)	1.49 (1)	P(1)-F(4′)	1.543 (9)	1.580 (3)
N(3)-C(7)	1.469 (6)	1.46 (1)	P(1)-F(5′)	1.570 (6)	1.489 (3)
N(3)-C(8)	1.475 (6)	1.45 (1)	P(1)-F(6′)	1.526 (7)	1.452 (3)
N(4)-C(9)	1.476 (6)	1.48 (1)			
N(4)-C(10)	1.326 (5)	1.34 (1)			
C(1)-C(2)	1.362 (6)	1.32 (1)			
C(1)-C(1M)	1.519 (7)	1.58 (1)			
C(2)-C(3)	1.436 (6)	1.40 (1)			
C(3)-C(3M)	1.523 (7)	1.58 (1)			
C(4)-C(5)	1.532 (7)	1.50 (1)			

B. $[Fe(sal)_2trien]Cl\cdot H_2O$ and $[Fe(sal)_2trien]NO_3\cdot H_2O$ (*C* and *D*, Respectively)

	C	*D*		*C*	*D*
Fe-OA	1.890 (1)	1.892 (2)	C(1)-C(2)	1.407 (3)	1.407 (4)
Fe-OB	1.878 (1)	1.872 (2)	C(1)-C(6)	1.415 (3)	1.408 (4)
Fe-N(1)	1.929 (2)	1.930 (2)	C(1)-C(7)	1.436 (3)	1.437 (4)
Fe-N(2)	2.003 (2)	2.000 (3)	C(2)-C(3)	1.406 (3)	1.406 (4)
Fe-N(3)	2.009 (2)	1.998 (3)	C(3)-C(4)	1.370 (3)	1.370 (4)
Fe-N(4)	1.931 (2)	1.934 (2)	C(4)-C(5)	1.375 (4)	1.385 (5)
OA-C(2)	1.322 (2)	1.329 (3)	C(5)-C(6)	1.365 (3)	1.359 (5)
OB-C(2B)	1.321 (3)	1.315 (3)	C(8)-C(9)	1.510 (3)	1.515 (5)
N(1)-C(7)	1.282 (3)	1.271 (4)	C(10)-C(11)	1.506 (4)	1.494 (5)
N(1)-C(8)	1.473 (3)	1.479 (4)	C(12)-C(13)	1.515 (3)	1.513 (5)
N(2)-C(9)	1.487 (3)	1.482 (4)	C(1B)-C(2B)	1.408 (3)	1.422 (4)
N(2)-C(10)	1.481 (3)	1.487 (4)	C(1B)-C(6B)	1.419 (3)	1.407 (4)
N(3)-C(11)	1.492 (3)	1.495 (4)	C(1B)-C(7B)	1.430 (3)	1.429 (4)
N(3)-C(12)	1.484 (3)	1.491 (4)	C(2B)-C(3B)	1.404 (3)	1.398 (4)
N(4)-C(13)	1.468 (3)	1.445 (4)	C(3B)-C(4B)	1.386 (4)	1.365 (4)
N(4)-C(7B)	1.288 (3)	1.268 (4)	C(4B)-C(5B)	1.377 (4)	1.395 (5)
			C(5B)-C(6B)	1.365 (4)	1.352 (5)
N-OD		1.198 (6)	N-OG		1.33 (2)
N-OE		1.27 (2)	N-OH		1.35 (8)
N-OF		1.22 (4)	N-OI		1.3 (1)

factors are available.[29]

Final positional and thermal parameters are given in Table III. Tables IV and V contain the bond lengths and angles. The digits in parentheses in the tables are the estimated standard deviations in the least significant figures quoted and were derived from the inverse matrix in the course of least-squares refinement calculations. Figure 4 is a stereoscopic pair view of the $[Fe(acac)_2trien]^+$ ion of the $[Fe(acac)_2trien]PF_6$ compound, while Figure 5 shows the packing diagram. $[Fe(acacCl)_2trien]^+$ has a very similar structure and is therefore not shown in detail beyond that given in Figure 1. Figure 6 is a stereopair view of the $[Fe(sal)_2trien]^+$ ion in the $[Fe(sal)_2trien]Cl\cdot 2H_2O$ compound, and Figure 7 shows the molecular packing of the complex in the unit cell, including hydrogen bonding links involving the cation, the chloride anion, and the two water molecules. Figure 8 is a stereopair view of the molecular packing in $[Fe(sal)_2trien]NO_3\cdot H_2O$ showing the principal position of the nitrate ion and the hydrogen bonding linking the water molecule to the two ions.

$[Fe(acac)_2trien]PF_6$. The lattice of this complex consists of well-defined $[Fe(acac)_2trien]^+$ ions and disordered PF_6^- ions. The complex cations are separated from one another by the PF_6^- anions (Table VI), the closest interionic approaches being 3.06 [F(3′) to N(3)] and 3.08 [F(4′) to C(8)]. The disorder in the PF_6^- group is essentially axial, consisting of two positions separated by a rotation of about 45° about the F(1)-P-F(2) axis. The disorder is not entirely accounted for by these positions, but the remaining positions contribute significantly less electron density than the hydrogen positions in the molecules. Since the complex cation is well defined, and the PF_6^- ion was not of primary interest, this disorder problem was not pursued further. The metal environment in the complex cation is approximately octahedral, with the two terminal oxygen atoms cis to each other. The deviation from octahedral symmetry of the FeN_4O_2 unit is indicated by bond lengths, angles, and interplanar angles. The angles O(1)-Fe-N(2), O(2)-Fe-N(3), and N(1)-Fe-N(4) all deviate markedly from the ideal octahedral 180° (161.0, 160.6, and 173.5°, respectively). The metal-ligand bond lengths are uneven: the two Fe-O bonds are by far the shortest (1.930 Å average), and the bonds to the amino nitrogen atoms are longer (2.174 Å) than those to the imino nitrogens (2.098 Å). The 12 angles subtended at the

Table V. Bond Angles (deg)

A. $[Fe(acac)_2trien]PF_6$ and $[Fe(acacCl)_2trien]PF_6$ (*A* and *B*, Respectively)

	A	*B*		*A*	*B*
O(1)-Fe-O(2)	102.1 (1)	99.7 (3)	Fe-N(3)-C(7)	110.1 (3)	110.0 (6)
O(1)-Fe-N(1)	87.9 (1)	85.5 (3)	Fe-N(3)-C(8)	104.9 (3)	103.4 (6)
O(1)-Fe-N(2)	161.0 (1)	161.4 (3)	C(7)-N(3)-C(8)	113.3 (4)	115.3 (8)
O(1)-Fe-N(3)	92.2 (1)	93.3 (3)	Fe-N(4)-C(9)	116.5 (3)	114.4 (6)
O(1)-Fe-N(4)	95.0 (1)	97.4 (3)	Fe-N(4)-C(10)	125.8 (3)	128.8 (6)
O(2)-Fe-N(1)	97.2 (1)	97.3 (3)	C(9)-N(4)-C(10)	117.4 (4)	116.6 (8)
O(2)-Fe-N(2)	91.0 (1)	92.3 (3)	1o)1)-C(1)-C(2)	124.1 (4)	122 (1)
O(2)-Fe-N(3)	160.6 (1)	161.2 (3)	O(1)-C(1)-C(1M)	114.6 (4)	109.9 (9)
O(2)-Fe-N(4)	87.9 (1)	86.7 (3)	C(2)-C(1)-C(1M)	120.2 (5)	128 (1)
N(1)-Fe-N(2)	76.7 (1)	78.9 (3)	Cl(1)-C(2)-C(1)		116.1 (9)
N(1)-Fe-N(3)	96.5 (1)	97.1 (3)	Cl(1)-C(2)-C(3)		114.3 (8)
N(1)-Fe-N(4)	173.5 (1)	174.7 (3)	C(1)-C(2)-C(3)	125.1 (5)	130 (1)
N(2)-Fe-N(3)	78.8 (1)	78.8 (3)	N(1)-C(3)-C(2)	123.4 (4)	120 (1)
N(2)-Fe-N(4)	99.3 (1)	97.5 (3)	N(1)-C(3)-C(3M)	120.2 (4)	119.4 (9)
N(3)-Fe-N(4)	77.6 (1)	78.2 (3)	C(2)-C(3)-C(3M)	116.5 (5)	121 (1)
Fe-O(1)-C(1)	130.1 (3)	131.1 (6)	N(1)-C(4)-C(5)	109.2 (4)	110.9 (9)
Fe-O(2)-C(12)	131.7 (3)	131.9 (7)	N(2)-C(5)-C(4)	108.4 (4)	111.5 (9)
Fe-N(1)-C(3)	125.1 (3)	127.4 (7)	N(2)-C(6)-C(7)	108.1 (4)	107.7 (9)
Fe-N(1)-C(4)	116.1 (3)	112.9 (6)	N(3)-C(7)-C(6)	108.3 (4)	110.9 (9)
C(3)-N(1)-C(4)	117.9 (4)	119.0 (8)	N(3)-C(8)-C(9)	110.7 (4)	112.4 (8)
Fe-N(2)-C(5)	105.3 (3)	103.0 (6)	N(4)-C(9)-C(8)	107.9 (4)	109.9 (9)
Fe-N(2)-C(6)	109.7 (3)	109.7 (6)	N(4)-C(10)-C(11)	123.7 (4)	118.1 (9)
C(5)-N(2)-C(6)	114.5 (4)	113.9 (8)	N(4)-C(10)-C(10M)	121.5 (4)	122.2 (9)
C(11)-C(10)-C(10M)	114.8 (4)	120 (1)	F(1)-P(1)-F(3′)	80.3 (6)	84.2 (1)
C(10)-C(11)-C(12)	124.0 (5)	129 (1)	F(1)-P(1)-F(4′)	80.1 (6)	72.6 (1)
O(2)-C(12)-C(11)	125.9 (5)	125 (1)	F(1)-P(1)-F(5′)	100.9 (4)	104.3 (2)
O(2)-C(12)-C(12M)	114.2 (4)	113.3 (9)	F(1)-P(1)-F(6′)	96.0 (4)	104.7 (2)
C(11)-C(12)-C(12M)	119.9 (5)	122 (1)	F(2)-P(1)-F(3′)	104.5 (6)	99.5 (2)
F(1)-P(1)-F(2)	175.1 (2)	176.3 (2)	F(2)-P(1)-F(4′)	98.4 (6)	107.8 (2)
F(1)-P(1)-F(3)	105.3 (5)	111.3 (2)	F(2)-P(1)-F(5′)	74.3 (3)	72.2 (1)
F(1)-P(1)-F(4)	87.4 (5)	87.8 (2)	F(2)-P(1)-F(6′)	85.6 (4)	75.1 (1)
F(1)-P(1)-F(5)	74.5 (4)	75.4 (1)	F(3′)-P(1)-F(4′)	91.4 (7)	86.1 (1)
F(1)-P(1)-F(6)	94.5 (5)	85.4 (2)	F(3′)-P(1)-F(5′)	177.5 (6)	165.5 (2)
F(2)-P(1)-F(3)	78.7 (5)	72.1 (1)	F(3′)-P(1)-F(6′)	86.8 (5)	90.8 (2)
F(2)-P(1)-F(4)	89.9 (5)	90.5 (2)	F(4′)-P(1)-F(5′)	86.7 (6)	85.3 (2)
F(2)-P(1)-F(5)	101.9 (4)	101.5 (2)	F(4′)-P(1)-F(6′)	175.9 (7)	176.0 (2)
F(2)-P(1)-F(6)	88.4 (5)	96.4 (2)	F(5′)-P(1)-F(6′)	95.3 (5)	98.2 (2)
F(3)-P(1)-F(4)	88.2 (6)	94.8 (2)	Cl(2)-C(11)-C(10)		115.8 (9)
F(3)-P(1)-F(5)	172.7 (4)	167.7 (2)	Cl(2)-C(11)-C(12)		115.7 (9)
F(3)-P(1)-F(6)	89.4 (5)	85.2 (1)			
F(4)-P(1)-F(5)	99.1 (6)	95.8 (2)			
F(4)-P(1)-F(6)	177.3 (6)	172.7 (2)			
F(5)-P(1)-F(6)	83.4 (5)	85.1 (1)			

B. $[Fe(sal)_2trien]Cl\cdot 2H_2O$ and $[Fe(sal)_2trien]NO_3\cdot H_2O$ (*C* and *D*, Respectively)

	C	*D*		*C*	*D*
OA-Fe-OB	93.98 (6)	93.83 (9)	Fe-N(3)-C(11)	110.3 (1)	110.6 (2)
OA-Fe-N(1)	93.44 (7)	93.0 (1)	Fe-N(3)-C(12)	108.1 (2)	108.4 (2)
OA-Fe-N(2)	175.32 (7)	175.7 (1)	C(11)-N(3)-C(12)	115.4 (2)	114.6 (3)
OA-Fe-N(3(	91.55 (7)	92.0 (1)	Fe-N(4)-C(13)	115.3 (1)	115.6 (2)
OA-Fe-N(4)	87.25 (6)	86.58 (9)	Fe-N(4)-C(7B)	125.0 (2)	123.3 (2)
OB-Fe-N(1)	88.50 (7)	87.9 (1)	C(13)-N(4)-C(7B)	119.5 (2)	120.8 (3)
OB-Fe-N(2)	89.80 (7)	89.4 (1)	C(2)-C(1)-C(6)	119.3 (2)	119.4 (3)
OB-Fe-N(3)	173.77 (7)	173.6 (1)	C(2)-C(1)-C(7)	123.1 (2)	122.6 (3)
OB-Fe-N(4)	93.37 (7)	94.2 (1)	C(6)-C(1)-C(7)	117.6 (2)	118.0 (3)
N(1)-Fe-N(2)	83.88 (7)	84.3 (1)	OA-C(2)-C(1)	123.8 (2)	124.0 (3)
N(1)-Fe-N(3)	94.03 (7)	94.5 (1)	OA-c)2)-C(3)	118.7 (2)	118.7 (3)
N(1)-Fe-N(4)	177.96 (7)	177.9 (1)	C(1)-C(2)-C(3)	117.5 (2)	117.2 (3)
N(2)-Fe-N(3)	84.82 (8)	85.0 (1)	C(2)-C(3)-C(4)	121.5 (2)	121.8 (3)
N(2)-Fe-N(4)	95.29 (7)	96.0 (1)	C(3)-C(4)-C(5)	121.1 (2)	120.8 (3)
N(3)-Fe-N(4)	84.03 (7)	83.5 (1)	C(4)-C(5)-C(6)	119.2 (2)	118.8 (3)
Fe-OA-C(2)	125.7 (1)	125.1 (2)	C(1)-C(6)-C(5)	121.4 (2)	122.0 (3)
Fe-OB-C(2B)	125.0 (1)	125.9 (2)	N(1)-C(7)-C(1)	125.0 (2)	125.2 (3)
Fe-N(1)-C(7)	125.7 (1)	126.0 (2)	N(1)-C(8)-C(9)	105.8 (2)	106.3 (3)
Fe-N(1)-C(8)	115.0 (1)	114.2 (2)	N(2)-C(9)-C(8)	108.5 (2)	108.5 (3)
C(7)-N(1)-C(8)	119.2 (2)	119.6 (3)	N(2)-C(10)-C(11)	110.0 (2)	109.6 (3)
Fe-N(2)-C(9)	107.1 (2)	108.4 (2)	N(3)-C(11)-C(10)	110.3 (2)	110.7 (3)
Fe-N(2)-C(10)	111.5 (1)	110.9 (2)	N(3)-C(12)-C(13)	109.6 (2)	108.2 (3)
C(9)-N(2)-C(10)	115.1 (2)	115.0 (3)	N(4)-C(13)-C(12)	106.1 (2)	107.3 (3)
C(2B)-C(1B)-C(6B)	119.4 (2)	118.3 (3)	C(2B)-C(3B)-C(4B)	120.9 (3)	122.2 (3)
C(2B)-C(1B)-C(7B)	122.8 (2)	122.3 (3)	C(3B)-C(4B)-C(5B)	120.9 (3)	120.4 (3)

Table V (*Continued*)

	B. $[Fe(sal)_2trien]Cl\cdot 2H_2O$ and $[Fe(sal)_2trien]NO_3\cdot H_2O$ (*C* and *D*, Respectively)				
	C	*D*		*C*	*D*
C(6B)-C(1B)-C(7B)	117.8 (2)	119.4 (3)	C(4B)-C(5B)-C(6B)	119.7 (2)	118.8 (3)
OB-C(2B)-C(1B)	124.4 (2)	123.3 (3)	C(1B)-C(6B)-C(5B)	121.1 (3)	122.7 (4)
OB-C(2B)-C(3B)	117.5 (2)	119.1 (3)	N(4)-C(7B)-C(1B)	124.9 (2)	127.2 (3)
C(1B)-C(2B)-C(3B)	118.1 (2)	117.6 (3)			
OD-N-OE		116.3 (9)	OE-N-OF		120 (2)
OD-N-OF		122 (2)	OE-N-OI		129 (5)
OD-N-OG		114 (1)	OF-N-OG		120 (2)
OD-N-OH		120 (3)	OG-N-OH		127 (3)
OD-N-OI		111 (4)			

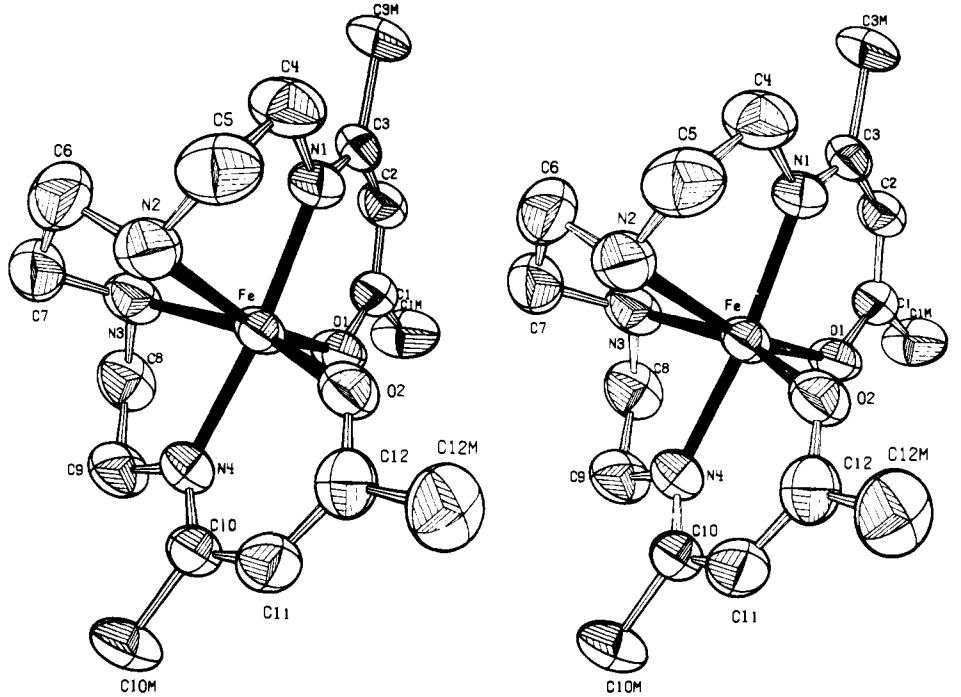

Figure 4. Stereopair view of the $[Fe(acac)_2trien]^+$ cation in $[Fe(acac)_2trien]PF_6$.

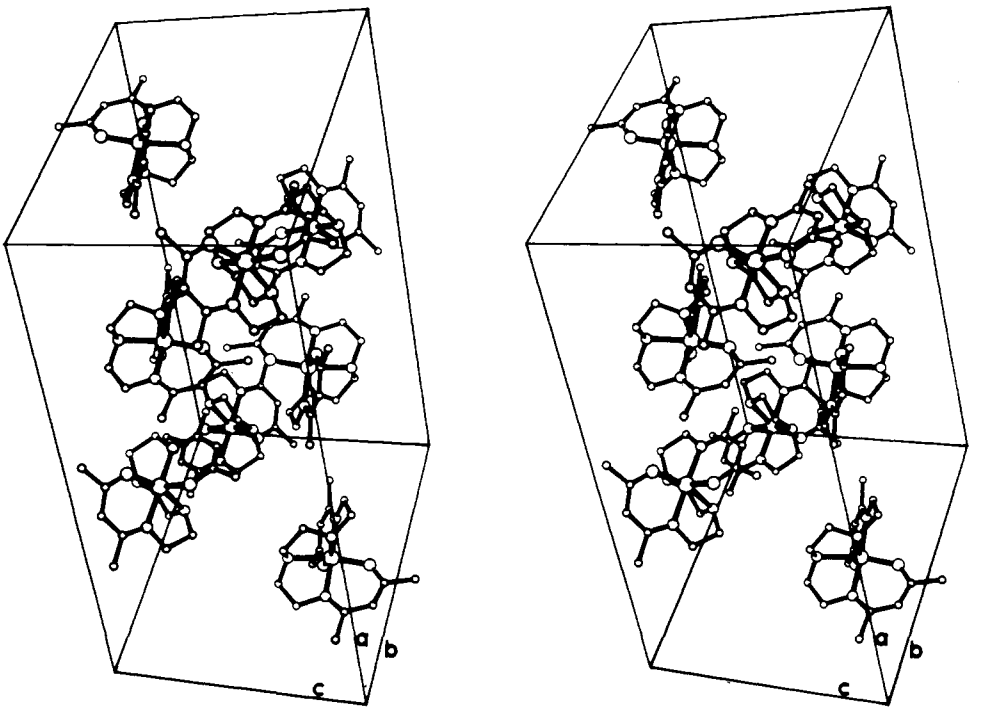

Figure 5. Stereopair view of the molecular packing for the $[Fe(acac)_2trien]PF_6$ complex.

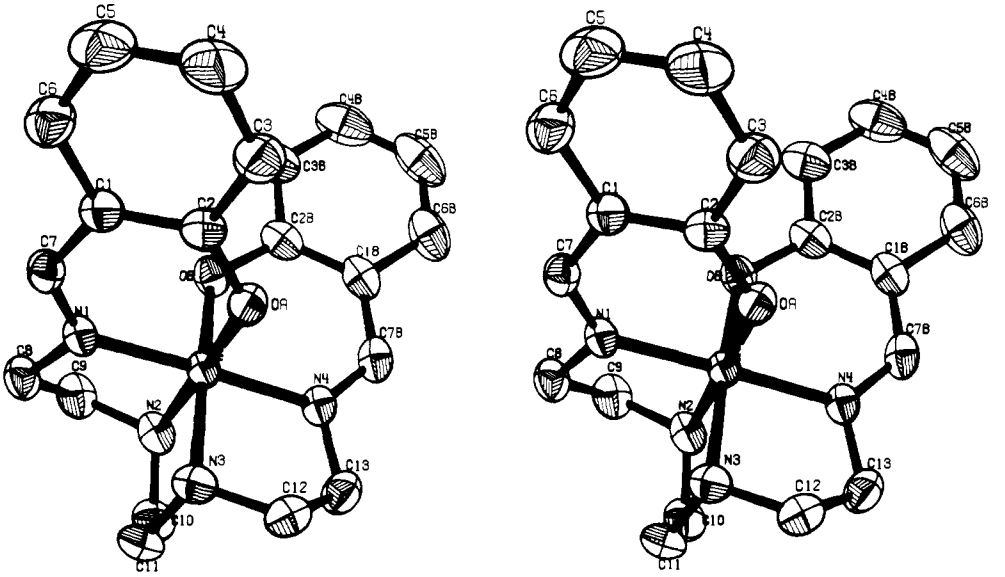

Figure 6. Stereopair view of the $[Fe(sal)_2trien]^+$ cation in $[Fe(sal)_2trien]Cl\cdot 2H_2O$.

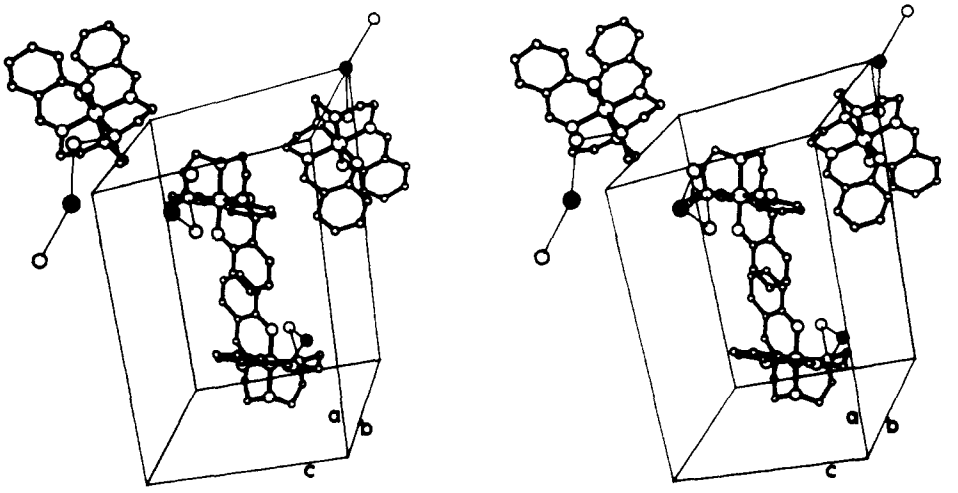

Figure 7. Stereopair view of the molecular packing for the $[Fe(sal)_2trien]Cl\cdot 2H_2O$ complex.

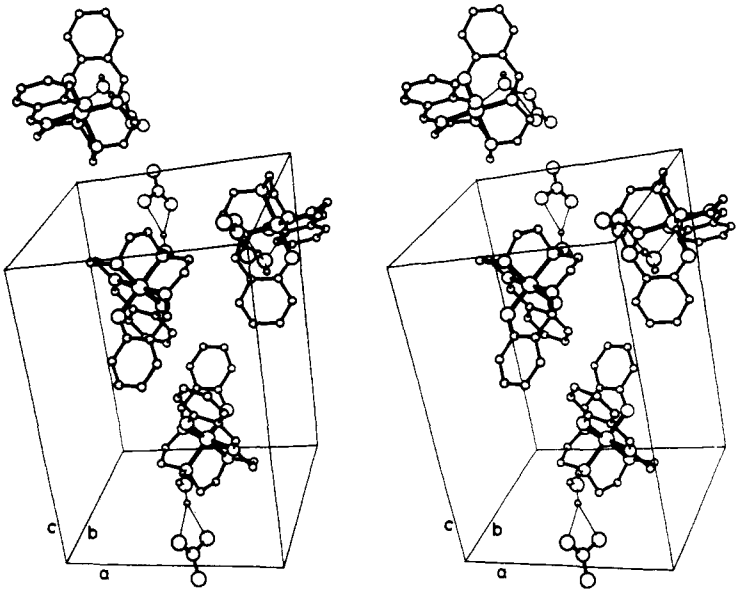

Figure 8. Stereopair view of the molecular packing for the $[Fe(sal)_2trien]NO_3\cdot H_2O$ complex.

Table VI. Intermolecular or Interion Contacts (Å)

Mol 1	Mol 2	Distance, Å: $[Fe(acac)_2trien]PF_6$	Distance, Å: $[Fe(acacCl)_2trien]PF_6$	Symmetry transformation		
Cl(1)	C(10)M		3.37 (1)	x	$-y$	$\frac{1}{2}+z$
Cl(2)	Cl(2)		3.04 (1)	$-x$	y	$-\frac{1}{2}-z$
F(1)	C(9)	3.19	3.30 (1)	$\frac{1}{2}-x$	$\frac{1}{2}+y$	$\frac{1}{2}-z$
F(3)	N(3)	3.15	3.26 (3)	$\frac{1}{2}-x$	$\frac{1}{2}-y$	$\frac{1}{2}+z$
	C(3)	3.22	3.25 (2)	$\frac{1}{2}-x$	$\frac{1}{2}-y$	$\frac{1}{2}+z$
F(4)	C(6)	3.23	3.40 (3)	x	y	z
F(5)	N(2)	3.38	3.22 (2)	x	$1-y$	$\frac{1}{2}+z$
	C(10)	3.16	3.06 (1)	x	$1-y$	$\frac{1}{2}+z$
	C(12)M	3.28	3.25 (2)	$-x$	y	$\frac{1}{2}+z$
F(6)	N(3)	3.10	2.92 (2)	$\frac{1}{2}-x$	$\frac{1}{2}-y$	$\frac{1}{2}+z$
	C(6)	3.28	3.52 (2)	$\frac{1}{2}-x$	$\frac{1}{2}-y$	$\frac{1}{2}+z$
F(3′)	N(3)	3.06	3.02 (2)	$\frac{1}{2}-x$	$\frac{1}{2}-y$	$\frac{1}{2}+z$
	C(2)	3.31	3.21 (2)	$\frac{1}{2}-x$	$\frac{1}{2}-y$	$\frac{1}{2}+z$
	C(3)	3.35	3.18 (3)	$\frac{1}{2}-x$	$\frac{1}{2}-y$	$\frac{1}{2}+z$
F(4′)	C(8)	3.08	3.28 (4)	$\frac{1}{2}-x$	$\frac{1}{2}+y$	$\frac{1}{2}-z$
F(5′)	C(4)	3.20	3.40 (3)	x	y	z
	C(12)M	3.29	3.27 (3)	$-x$	y	$\frac{1}{2}-z$
F(6′)	N(2)	3.12	3.29 (2)	x	$1-y$	$\frac{1}{2}+z$

$[Fe(sal)_2trien]NO_3 \cdot H_2O$ Hydrogen Contacts

Atom 1	H atom	Atom 2	D^a	d^b	Symmetry		
N(2)	HN(2)	OC	2.908	2.04	x	y	z
OC	HOC(1)	OD	2.984 (4)	2.12	x	$y-1$	$z-1$
OC	HOC(1)	OE	2.94 (1)	2.13	x	$y-1$	$z-1$
N(3)	HN(3)	OD	3.005 (4)	2.07	x	y	$z-1$
N(3)	HN(3)	OF	3.13 (3)	2.36	x	y	$z-1$

$[Fe(sal)_2trien]Cl \cdot H_2O$ Hydrogen Contacts

N(2)	HN(2)	OC	2.929 (3)	2.10	x	y	z
N(3)	HN(3)	Cl	3.261 (2)	2.44	x	$1+y$	z
OC	HC)1)	Cl	13.13	2.09	x	y	z
OD	HD(1)	Cl	3.297 (2)	2.32	x	y	z

[a] Atom 1 to atom 2. [b] H atom to atom 2.

metal atom by adjacent donor atoms range from 76.7 to 102.1°, compared to the 90° required for a perfect octahedron. The three planes defined by the three groups of four equatorial ligand donor atoms deviate somewhat from true planarity (planes I-III in Table VII, available elsewhere[29]), but are nearly orthogonal to each other. The iron atom lies 0.15 and 0.16 Å, respectively, above the planes (II) O(1)N(1)N(2)N(4) and (III) O(2)N(1)N(3)N(4). Thus, the main deviation from octahedral geometry consists of a shift of the metal atom from the center of the ligand octahedron. The keto imine ligand fragments bend sharply away from the appropriate equatorial planes II and III.

$[Fe(acacCl)_2trien]PF_6$. The structure of this compound is quite similar to that of $[Fe(acac)_2trien]PF_6$, as expected. Some differences in the bond lengths and angles in the acac rings in the two compounds may be due to the chlorine substitution on the acac backbone, but the differences cannot be measured accurately because of the relatively low accuracy of the $[Fe(acacCl)_2trien]PF_6$ data set. Again, the angles O(1)-Fe-N(2), O(2)-Fe-N(3), and N(1)-Fe-N(4) deviate considerably from 180° (161.4, 161.2, 174.7°). The metal-ligand bond lengths are asymmetric, the Fe-O bonds being the shortest (1.908 Å), followed by the Fe-imine (2.096 Å) and Fe-amine (2.173 Å) nitrogen bonds. The angles subtended by adjacent donor atoms at the Fe range as widely as for the $[Fe(acac)_2trien]^+$ ion. The three equatorial planes deviate a little from being orthogonal to one another (Table VII),[29] and, as with the acac analogue, the main deviation from octahedral symmetry is the shift of the iron atom from the center of the octahedron. The keto imine fragments of the ligand again bend away from the adjacent equatorial planes.

$[Fe(sal)_2trien]Cl \cdot 2H_2O$. The lattice of this complex contains closely linked cations, anions, and water molecules; the closest interionic and intermolecular approaches are given in Table VI. The $[Fe(sal)_2trien]^+$ ion is hydrogen bonded via an amine nitrogen [HN(2), attached to the nitrogen atom N(2)], to one of the water molecules (OC), which in turn is hydrogen bonded [via HC(1), attached to OC] to the chloride anion. The chloride anion is in turn more weakly hydrogen bonded to the other water molecule [via HD(1), attached to OD], and to the other amine nitrogen of another cation [via HN(3) attached to N(3)]. This hydrogen bonding network connects adjacent $[Fe(sal)_2trien]^+$ ions separated by one unit cell translation along the *b* axis to form infinite chains of hydrogen-bonded ions and water molecules, -cation-water-anion-cation-, etc.

Owing to the extensive hydrogen bonding, the positions of the anion and the lattice water molecules (and the hydrogen atoms associated with them) are very well defined, and this, together with excellent crystal quality, enabled a very accurate x-ray data set to be obtained. The first coordination sphere around the metal atom in the complex cation is approximately octahedral with the two terminal oxygen atoms cis to each other. The configuration of the hexadentate ligand about the metal atom is analogous to that of $(acac)_2trien$ and $(acacCl)_2trien$ in the other two complexes, but the deviation of the FeN_4O_2 unit from octahedral geometry is much smaller. The angles OA-Fe-N(2), OB-Fe-N(3), and N(1)-Fe-N(4) are all quite close to 180° (175.3, 173.8, 178.0°) and the metal-ligand bond lengths are uneven but markedly less so than in $[Fe(acac)_2trien]PF_6$ and $[Fe(acac)_2trien]PF_6$. The bonds to the oxygen atoms are the shortest (1.884 Å) followed by those to the imine (1.930 Å) and the amine (2.006 Å) nitrogen atoms. The difference in the bonds linking the iron to the amine nitrogen atoms (0.006 Å) is significant, and may be a function of the different types of hydrogen bonding to these nitrogens. In fact, the N-H(st) region in the infrared spectrum for this

compound apparently reflect the nonequivalency of the two N-H groups in showing at least six distinct N-H and O-H stretching frequencies.[16] The 12 angles subtended at the iron atom by adjacent donor atoms are approximate right angles, ranging from 84.0 to 95.3°. The three equatorial planes are less nearly orthogonal (Table VII) than in the $[Fe(acac)_2trien]^+$ and $[Fe(acacCl)_2trien]^+$, ions, but the iron atom is close to the center of the ligand octahedron. To a lesser extent than in the $[Fe(acac)_2trien]^+$ and $[Fe(acacCl)_2trien]^+$ ions, the imine nitrogen-oxygen chelate rings bend at the donor atoms but are almost coplanar with the attached phenyl rings.

$[Fe(sal)_2trien]NO_3 \cdot H_2O$. Like the chloride analogue, the lattice of this compound contains closely linked cations, anions, and water molecules; the closest interionic and intermolecular approaches are given in Table VI. The $[Fe(sal)_2trien)]^+$ ion is hydrogen bonded via an amine nitrogen [HN(2) attached to the nitrogen atom N(2)], to the water molecule OC which is in turn hydrogen bonded [via HOC(1) attached to OC] to oxygen atom OD of the nitrate anion. The nitrate ion is hydrogen bonded to an amine ligand nitrogen atom [via HN(3) attached to N(3)] of the next cation. As in the chloride analogue, this produces an infinite hydrogen-bonded chain along the *b* axis. The nitrate anion exhibits positional disorder, principally by rotation about the N-OD bond. Strong hydrogen bonding to OD prevents positional disorder of this atom. The disordered nitrate positions are listed in Table III. The first coordination sphere about the metal atom is approximately octahedral with cis terminal oxygen atoms. The configuration of the hexadentate ligand is analogous to the other three complexes. As in $[Fe(sal)_2trien]Cl \cdot 2H_2O$, the distortion of the FeN_4O_2 from octahedral geometry is much smaller than in the acac-based complexes. The angles OA-Fe-N(2), OB-Fe-N(3), and N(1)-Fe-N(2) are all quite close to 180° (175.7, 173.6, 177.9°) and the iron atom is near the center of the ligand octahedron. The metal-ligand bond lengths are uneven, like the chloride analogue, but markedly less so than the acac-based complexes. The bonds to the oxygen atoms are the shortest (1.882 Å), followed by those to the imine (1.932 Å) and the amine (1.999 Å) nitrogen atoms. Despite the existence of the hydrogen bonding between the water molecules and ligand atom N(2), elongation of the Fe-N(2) bond length is quite negligible when compared to the Fe-N(3) bond (1.998 Å), which is affected by weaker hydrogen bonding to the nitrate ion. The 12 angles subtended at the iron atom by adjacent donor atoms are approximate right angles ranging from 83.5 to 96.0°.

All four structures, and those of the $[Fe(sal)_2trien]^+$ ions in particular, may be compared with the structure of the only other sal_2trien complex so far studied by x-ray diffraction, $[Ni(sal)_2trien] \cdot 6H_2O$.[34] The nickel complex has the same configuration of the hexadentate ligand as in the four iron complexes, and the NiN_4O_2 unit deviates much more from octahedral geometry than FeN_4O_2 in $[Fe(sal)_2trien]^+$ but not nearly as much as FeN_4O_2 in $[Fe(acac)_2trien]PF_6$ and $[Fe(acacCl)_2trien]PF_6$. For example, the corresponding "linear" angles are 164.4, 164.4, and 177.4° in $[Ni(sal)_2trien]$, and the angles subtended at the nickel atom by adjacent ligands range from 80.4 to 101.6°. The nickel to ligand (amine 2.159 Å, imine 2.029 Å) bond lengths lie between those of the high-spin (acac) and low-spin (sal) iron complexes, except for the anomalously long Ni-O bonds (2.038 Å) which are perturbed by hydrogen bonding to water molecules. The data suggest that the two ligands are highly similar in their steric requirements and that the distortion from octahedral geometry increases in each case with increasing metal-ligand bond lengths. However, the hydrogen bonding to the ligand oxygen atoms in the nickel complex adds an element of uncertainty so that the extent of the slight differences in steric requirements between the two ligands cannot yet be quantified. The distortion from octahedral geometry of the type observed in all three iron complexes would be expected to induce term state splittings ($^2T_2$ would split to ^2A and ^2E, with further splitting of the ^2E) and increase the probability of spin state equilibria.[9,10]

The complexes $[Fe(acac)_2trien]PF_6$ and $[Fe(acacCl)_2trien]PF_6$ are almost entirely high spin in the solid state at room temperature, whereas $[Fe(sal)_2trien]Cl \cdot 2H_2O$ and $[Fe(sal)_2trien]NO_3 \cdot H_2O$ are essentially low spin around room temperature. There are obvious differences between the two types of ligands used to obtain the high-spin and low-spin complexes, respectively, such as the extent of electron delocalization in the sal and acac moieties. However, within the limits that it can so far be determined, these differences play a relatively minor role in determining the actual coordination geometry and spin state, since both types of ligands produce varying proportions of high-spin and low-spin species depending on the counterion and degree of hydration. Counterion dependence of spin-equilibrium phenomena in the solid are well documented;[39] however, the specific $[H_2O \cdots HN\text{-}Fe(III)]$ hydrogen bonding pattern found in the $[Fe(sal)_2trien]^+$ structures is clearly an important factor in producing the low-spin state in these complexes, as was suggested earlier from the solution state studies[16] where solvents producing the strongest [S···HN] hydrogen bonding interactions also produced the greatest low-spin isomer populations.

The average metal-ligand distances in the two high-spin complexes, r_h, are 2.059 and 2.068 Å, whereas in the low-spin complex, the distances, r_l, are 1.940 and 1.939 Å. This gives an average difference, δ, between the essentially high-spin and low-spin forms of at least 0.124 Å. Use of only the 2.068 Å value of r_h (from the more accurate $[Fe(acac)_2trien]^+$ data) would give a value closer to 0.13 Å for δ. It is instructive to compare this result with other spin state dependent structural information available for the most studied of the $3d^5$ systems—that for the tris(dithiocarbamato)iron(III) complexes. From the molar volume change ΔV, measured in solution, between high-spin and low-spin forms, it is possible to calculate the difference, δ, between r_h and r_l, using the relationship

$$\Delta V = 4\pi N r_h r_l \delta \qquad (1)$$

or $\Delta V = 7.57 r_h r_l \delta$, if ΔV is in cm^3/mol and the distances are in ångstroms. The experimental range of ΔV in ferric dithiocarbamates from high-pressure data was given as 5-6 cm^3/mol, with the higher values usually observed for the more accurate data, owing to solubility or inertia to formation of the inert chlorobis(dithiocarbamates) in chlorohydrocarbon solvents. Thus, 5.5 cm^3/mol appears to be a reasonable lower limit for ΔV. To convert the molar volume change to an average metal-ligand bond length change, it is necessary to define the radius r_l of the low-spin Fe-S_6 core of the dithiochelate, where the surface of the sphere passes through the averaged centers of the sulfur atoms (r_h is then $r_l + \delta$). Using an assumed value for r_l of 2.5 Å, in the absence of structural data, a δ value of 0.1 Å has been estimated.[1] An earlier[24] value of 0.08 Å from data on one complex was found to be an underestimate due to the lower experimental accuracy then available. From data on a range of ferric dithiochelates (Table VIII) the best available value for the low-spin Fe-S_6 radius (r_e) is 2.3 Å, which yields a value of 0.13 Å for δ from eq 1 and the literature high-pressure data.

A similar δ value of 0.13 Å can be estimated from the range of average Fe-S bond lengths determined by x-ray crystallography in a variety of ferric dithiochelates (Table VIII). The available data apply mainly to room temperature, with slightly different ligands, or with different solvent molecules included in the lattice and the same ligands. The four hexadentate complexes studied here indicate the same δ value of about 0.13 Å for the difference between pure high-spin and pure low-spin bond lengths, and based on this finding, a molar volume change

Table VIII. Magnetic Moments and Metal-Ligand Bond Lengths in Some High-Spin ($\mu_{eff} \simeq 5.9\ \mu_B$), Low-Spin ($\mu_{eff} \simeq 2.2\ \mu_B$), and Intermediate-Moment Iron(III) Complexes

Compd	μ_{eff}, μ_B	⟨Fe-S⟩, Å	Ref
Dithiochelate Complexes			
$Fe\{S_2CN(C_2H_5)_2\}_3$ (79 K)	2.2	2.306	13
$Fe\{S_2CSC(CH_3)_3\}_3$	2.5	2.297	36,37
$Fe\{S_2COC_2H_5\}_3$	2.7	2.316	38
$Fe\{S_2CN(CH_3)\cdot C_6H_5\}_3$	2.9	2.312	6
$FeM\cdot(C_6H_6)_2$	3.5	2.318	9
$Fe\{(S_2CN(n\text{-}C_4H_9)_2\}_3\cdot(C_6H_6)$	3.6	2.341	38
$Fe\{S_2CN(C_2H_5)_2\}_3$ (297 K)	4.3	2.357	13
$FeM\cdot CHCl_3$	5.5	2.416	10
$FeM\cdot CH_2Cl_2$	5.1	2.430	10
$Fe\{S_2CN(n\text{-}C_4H_9)_2\}_3$	5.3	2.42	5
$FeP\cdot(C_6H_6)_{1/2}$	5.6	2.434	15
$FeM\cdot(H_2O)$	5.6	2.443	10
FeP^a	5.9	2.41	6

	Hexadentate Complexes			
	μ_{eff}, μ_B	⟨Fe-N⟩, Å	⟨Fe-O⟩, Å	⟨Fe-lig⟩, Å
$[Fe(sal_2trien]NO_3\cdot H_2O$	2.5	1.966	1.882	1.939 (2)
$[Fe(sal)_2trien]Cl\cdot 2H_2O$	2.0	1.968	1.884	1.940 (2)
$[Fe(acacCl)_2trien]PF_6$	5.9	2.135	1.908	2.059 (7)
$[Fe(acac)_2trien]PF_6$	5.9	2.136	1.930	2.068 (3)

[a] Reference 42.

Table IX. Kinetic and Structural Data for the Spin-Equilibrium Iron Compounds

Compd	δ_{av}, Å[a]	k' (spin transition), s^{-1} [b]	Ref[c]
(1) $[Fe(III)(dtc)_3]^0$	Fe-S_6 (0.11)	$>2.0 \times 10^7$	13,17
(2) $[Fe(III)(sal)_2trien]^+$	Fe-N_4O_2 (0.13)	1.4×10^7	This work, 23b
(3) $[Fe(III)(acac)_2trien]^+$	Fe-N_4O_2 (0.13)	1.0×10^7	This work, 23b
(4) $[Fe(II)(6\text{-}Mepy)_2(py)tren]^{2+}$	Fe-N_6 (0.26)	4.5×10^6	19,25

[a] Estimated maximum in the ⟨Fe-ligand⟩ donor atom bond distance change upon spin transition. [b] k' is the average of k_1 and k_{-1} measured at room temperature, where $k' = (k_1k_{-1})^{1/2}$; experimental details are given in the references. [c] Structure and kinetics reference, respectively.

ΔV of 4 cm^3/mol is predicted for the spin transition in the hexadentate complexes.

The δ value of approximately 0.13 Å is general for (high spin) $\rightleftarrows$ (low spin) transitions in $3d^5$ systems (and their analogous electron pairing situations). A smaller δ value (0.09 Å) was recently reported for two tris(monothio-β-diketonato)-iron(III) complexes,[40] but these compounds do not represent pure high- and low-spin extremes and the δ value therefore represents a *lower* limit. A more precise determination of δ, and whether and how much it varies for different classes of compounds (such as Fe(hexadentate) and Fe(dtc) complexes), cannot yet be made from the limited data available.

Finally it should be noted that there is a continuing interest in ⟨metal-ligand⟩ bond distance changes in spin-equilibrium processes as they pertain to the measurement of spin state lifetimes in solution.[16,17,22,24,26] This subject has been recently addressed in detail elsewhere,[23b] where the spin multiplicity change is treated as an internal electron transfer reaction. Furthermore, it has been suggested that an important factor in determining intersystem crossing kinetics (k_1 and k_{-1})

$$\text{(low-spin)} \underset{k_{-1}}{\overset{k_1}{\rightleftarrows}} \text{(high spin)}$$

is the nature and extent of the primary coordination sphere reorganization process that accompanies the spin transition. In the extreme view, this ligand reorganization process could become the rate-determining factor, especially for cases where the ligand might offer large "mechanical restictions" to the changing geometry of the coordination sphere. It is felt that this is most likely to occur for multidentate ligands, such as the present hexadentates. At present, complementary structural and kinetic data are available for only the Fe(III)$(dtc)_3$'s, the $[Fe(III)(sal)_2trien]^+$ and $[Fe(III)(acac)_2trien]^+$ complexes, and for an iron(II) spin-equilibrium species, $[Fe(II)(6MePy)_n(Py)_mtren]^{2+}$.[19,25] Except for the $Fe(dtc)_3$ compounds, these complexes are all derived from hexadentate ligands, and it is precisely these species that display the "slower" intersystem crossing kinetics. The available structural and kinetic data for the three iron systems are summarized in Table IX.

Acknowledgment. Support received for instrumentation at the University of Virginia under NSF Grant GP-41679 is gratefully acknowledged. In addition, the NSF, the Robert A. Welch Foundation under Grant C-627, NASA under Materials Grant 44-006-001, and the donors of the Petroleum Research Fund, administered by the American Chemical Society, are gratefully acknowledged for work done at Rice University. Liquid helium for the magnetic susceptibility studies was obtained from the Helium Liquification Facility operated under Navy contract at Rice University.

Supplementary Material Available: (1) Listing of structure factor amplitudes; (2) variable-temperature magnetic susceptibility data from Table I; (3) least-squares planes from Table VII (42 pages). Ordering information is given on any current masthead page.

References and Notes

(1) University of Virginia.
(2) Rice University; Robert A. Welch Foundation Predoctoral Fellow.
(3) Rice University.
(4) A. H. Ewald, R. L. Martin, E. Sinn, and A. H. White, *Inorg. Chem.*, **8**, 1837

(1969).
(5) B. F. Hoskins and B. P. Kelley, *Chem. Commun.*, 1517 (1968).
(6) P. C. Healy and A. H. White, *J. Chem. Soc., Dalton Trans.*, 1163 (1972).
(7) B. F. Hoskins and B. P. Kelley, *Chem. Commun.*, 45 (1970).
(8) P. C. Healy and E. Sinn, *Inorg. Chem.*, **14**, 109 (1975).
(9) R. J. Butcher and E. Sinn, *J. Am. Chem. Soc.*, **98**, 2440 (1976).
(10) R. J. Butcher and E. Sinn, *J. Am. Chem. Soc.*, **98**, 5159 (1976).
(11) R. J. Butcher, J. R. Ferraro, and E. Sinn, *J. Chem. Soc., Chem. Commun.*, 910 (1976).
(12) E. J. Cukauskas, B. S. Deaver, Jr., and E. Sinn, *J. Phys. Chem.*, **67**, 1257 (1977); *Inorg. Nucl. Chem. Lett.*, **13**, 283 (1977).
(13) J. G. Leipoldt and P. Coppens, *Inorg. Chem.*, **12**, 2269 (1973).
(14) E. J. Cukauskas, E. Sinn, and B. S. Deaver, Jr., *Bull. Am. Phys. Soc.*, **19**, 229, 1120 (1974).
(15) E. Sinn, *Inorg. Chem.*, **15**, 369 (1976).
(16) M. F. Tweedle and L. J. Wilson, *J. Am. Chem. Soc.*, **98**, 4824 (1976).
(17) E. V. Dose, K. M. Murphy, and L. J. Wilson, *Inorg. Chem.*, **15**, 2622 (1976).
(18) E. König and K. J. Watson, *Chem. Phys. Lett.*, **6**, 457 (1970).
(19) M. A. Hoselton, L. J. Wilson, and R. S. Drago, *J. Am. Chem. Soc.*, **97**, 1722 (1975).
(20) L. J. Wilson, D. Georges, and M. A. Hoselton, *Inorg. Chem.*, **14**, 2968 (1975).
(21) See, for example, "Inorganic Compounds with Unusual Properties", *Adv. Chem. Ser.*, **No. 150**, 128–148 (1976).
(22) See, for example, E. V. Dose, M. F. Tweedle, L. J. Wilson, and N. Sutin, *J. Am. Chem. Soc.*, **99**, 3886 (1977).
(23) (a) K. R. Kunze, D. L. Perry, and L. J. Wilson, *Inorg. Chem.*, **16**, 594 (1977); (b) E. V. Dose, M. A. Hoselton, N. Sutin, M. F. Tweedle, and L. J. Wilson, *J. Am. Chem. Soc.*, **100**, 1141 (1978).
(24) J. K. Beattie, N. Sutin, D. H. Turner, and G. W. Flynn, *J. Am. Chem. Soc.*, **95**, 2053 (1973).
(25) M. A. Hoselton, R. S. Drago, L. J. Wilson, and N. Sutin, *J. Am. Chem. Soc.*, **98**, 6967 (1976).
(26) M. G. Simmons and L. J. Wilson, *Inorg. Chem.*, **16**, 126 (1977).
(27) C. J. O'Connor, E. J. Cukauskas, B. S. Deaver, Jr., and E. Sinn, submitted for publication.
(28) P. W. R. Corfield, R. J. Doedens, and J. A. Ibers, *Inorg. Chem.*, **6**, 197 (1967).
(29) See paragraph at end of paper regarding supplementary material.
(30) D. T. Cromer and J. T. Waber, "International Tables for X-Ray Crystallography", Vol. IV, Kynoch Press, Birmingham, England, 1974.
(31) R. F. Stewart, E. R. Davidson, and W. T. Simpson, *J. Chem. Phys.*, **42**, 3175 (1965).
(32) D. T. Cromer and J. T. Waber in ref 30.
(33) D. P. Freyberg, G. M. Mockler, and E. Sinn, *J. Chem. Soc., Dalton Trans.*, 447 (1976).
(34) P. D. Cradwick, M. E. Cradwick, G. G. Dodson, D. Hall, and T. N. Waters, *Acta Crystallogr., Sect. B*, **28**, 45 (1964).
(35) A. H. Ewald, R. L. Martin, I. G. Ross, and A. H. White, *Proc. R. Soc. London, Ser. A*, **280**, 235 (1964).
(36) A. H. Ewald and E. Sinn, *Aust. J. Chem.*, **21**, 927 (1968).
(37) D. F. Lewis, S. J. Lippard, and J. A. Zubieta, *Inorg. Chem.*, **11**, 823 (1972).
(38) B. F. Hoskins and B. P. Kelley, *Chem. Commun.*, 45 (1970).
(39) See, for example, H. A. Goodwin and R. N. Sylva, *Aust. J. Chem.*, **21**, 83 (1968); C. M. Harris, T. N. Lockyer, R. L. Martin, H. R. H. Patil, E. Sinn, and I. M. Stewart, *ibid.*, **22**, 2105 (1969).
(40) B. F. Hoskins and C. D. Pannan, *Inorg. Nucl. Chem. Lett.*, **11**, 409 (1975).
(41) M. F. Tweedle, and L. J. Wilson, *Rev. Sci. Instrum.*, in press.
(42) NOTE ADDED IN PROOF. New experimental data show that the anomalously short literature bond length (2.41 Å) in FeP (Table VIII) was indeed an underestimate (A. H. White, personal communication). Our own studies confirm this and show that the true high-spin FeP complex has a longer average Fe–S bond length (2.45 Å) at ambient and at low temperatures.

Electron Density in Bis(dicarbonyl-π-cyclopentadienyliron) at Liquid Nitrogen Temperature by X-Ray and Neutron Diffraction

André Mitschler,[1a] Bernard Rees,*[1a] and Mogens S. Lehmann[1b]

Contribution from the Institut de Chimie, Université Louis Pasteur, Laboratoire de Cristallochimie et Chimie Structurale, 67070 Strasbourg-Cédex, France, and the Institut Max von Laue-Paul Langevin, 38042 Grenoble-Cédex, France.
Received September 28, 1977

Abstract: The crystal structure of the title compound has been redetermined at 74 K, both by x-ray and by neutron diffraction, and electron deformation density maps have been computed by the *X–N* method. Practically no features significantly different from zero are observed in the region of the Fe–Fe bond. The asphericity of the electron density around the iron nuclei has been related to the unequal occupancy of the 3d metal orbitals, as indicated by a semiempirical molecular orbital calculation. The molecular geometry is also discussed, with particular emphasis on the distortions of the cyclopentadienyl rings.

Introduction

In many diamagnetic binuclear complexes, a single or multiple metal–metal bond is formally required in order for each metal atom to attain the closed-shell configuration implied by their magnetic behavior. But the nature of such a bond has given rise to numerous discussions, especially when the metals are bridged by ligands. A superexchange mechanism via the bridging ligands has been invoked.[2a] A direct proof of a distinct chemical bond has been given by Coleman and Dahl,[2b] in their structure determination of $[(C_6H_5)_2PCoC_5H_5]_2$ and of $[(C_6H_5)_2PNiC_5H_5]_2$: the effect of the electron spin-coupling interaction between the metals, which exists only in the former complex, is a decrease of the metal–metal distance from 3.36 Å in the nickel complex to 2.56 Å in the cobalt complex.

The investigation, from the point of view of the distribution of electron density, of such a metal–metal bond is reported here. Bis(dicarbonyl-π-cyclopentadienyliron) [more exactly, di-μ-carbonyldicarbonyl-bis(η^5-2,4-cyclopentadien-1-yl)di-iron], $[C_5H_5Fe(CO)_2]_2$, is a diamagnetic binuclear complex, with two carbonyl bridges, for which a single Fe–Fe bond is formally required from electron bookkeeping considerations. The crystal structures of both cis and trans isomers have been reported.[3-5] We have redetermined the crystal structure of the trans isomer at low temperature both by x-ray and neutron diffraction, in order to study the charge density by the so-called *X–N* method.

Experimental Section

Air-stable crystals of *trans*-$[(\pi\text{-}C_5H_5)Fe(CO)_2]_2$ were obtained by recrystallization of commercial material in an ethyl acetate solution under argon. Relevant crystal data are given in Table I. Since the unit cell contains two molecules, in space group $P2_1/c$, the midpoint of the Fe–Fe bond is necessarily a crystallographic inversion center. No indication of a structural phase change was found during cooling to liquid nitrogen temperature. The cell constants at 74 K were determined by a least-squares refinement of the diffractometer setting

0002-7863/78/1500-3390$01.00/0